STRATEGIC ANALYSIS INC

Mass Production Cost Estimation of Direct H_2 PEM Fuel Cell Systems for Transportation Applications: 2012 Update

October 18, 2012

Prepared By:

Brian D. James

Andrew B. Spisak

Revision 4

CREATIVE SOLUTIONS FOR TOMORROW'S CHALLENGES

STRATEGIC ANALYSIS INC

Sponsorship and Acknowledgements

This research was conducted under Award Number DE-EE0005236 to the US Department of Energy. The authors wish to thank Dr. Dimitrios Papageorgopoulos and Mr. Jason Marcinkoski of DOE's Office of Energy Efficiency and Renewable Energy (EERE) Fuel Cell Technologies (FCT) Program for their technical and programmatic contributions and leadership.

Authors Contact Information

Strategic Analysis Inc. may be contacted at:

Strategic Analysis Inc.
4075 Wilson Blvd, Suite 200
Arlington VA 22203
(703) 527-5410
www.sainc.com

The authors may be contacted at:

Brian D. James, BJames@sainc.com (703) 778-7114

Table of Abbreviations

ANL	Argonne National Laboratory
atm	atmospheres
BOL	Beginning of Life
BOM	Bill of Materials
BOP	Balance of Plant
CCM	catalyst coated membrane
CEM	Integrated Compressor-Expander-Motor unit (used for air compression and exhaust gas expansion)
DOE	Department of Energy
DOT	Department of Transportation
EERE	DOE Office of Energy Efficiency and Renewable Energy
EOL	end of life
ePTFE	expanded polytetrafluoroethylene
FCT	EERE Fuel Cell Technologies Program
FTA	Federal Transit Administration
GDL	Gas Diffusion Layer
H_2	Hydrogen
MEA	Membrane Electrode Assembly
mph	miles per hour
NREL	National Renewable Energy Laboratory
NSTF	nano-structured thin-film (catalysts)
PEM	Proton Exchange Membrane
PET	polyethylene terephthalate
RFI	Request for Information
SA	Strategic Analysis, Inc.
TVS	Twin Vortices Series (of Eaton Corp. compressors)

Foreword

Energy security is fundamental to the mission of the U.S. Department of Energy (DOE) and hydrogen fuel cell vehicles have the potential to eliminate the need for oil in the transportation sector. Fuel cell vehicles can operate on hydrogen, which can be produced domestically, emitting less greenhouse gasses and pollutants than conventional internal combustion engine (ICE), advanced ICE, hybrid, or plug-in hybrid vehicles that are tethered to petroleum fuels. A diverse portfolio of energy sources can be used to produce hydrogen, including nuclear, coal, natural gas, geothermal, wind, hydroelectric, solar, and biomass. Thus, fuel cell vehicles offer an environmentally clean and energy-secure transportation pathway for transportation.

Fuel cell systems will have to be cost-competitive with conventional and advanced vehicle technologies to gain the market-share required to influence the environment and reduce petroleum use. Since the light duty vehicle sector consumes the most oil, primarily due to the vast number of vehicles it represents, the DOE has established detailed cost targets for automotive fuel cell systems and components. To help achieve these cost targets, the DOE has devoted research funding to analyze and track the cost of automotive fuel cell systems as progress is made in fuel cell technology. The purpose of these cost analyses is to identify significant cost drivers so that R&D resources can be most effectively allocated toward their reduction. The analyses are annually updated to track technical progress in terms of cost and to indicate how much a typical automotive fuel cell system would cost if produced in large quantities (up to 500,000 vehicles per year).

Bus applications represent another area where fuel cell systems have an opportunity to make a national impact on oil consumption and air quality. Consequently, beginning with this year (2012), annually updated costs analyses will be conducted for PEM fuel cell passenger buses as well. Fuel cell systems for light duty automotive and buses share many similarities and indeed may even utilize identical stack hardware. Thus the analysis of bus fuel cell power plants is a logical extension of the light duty automotive power system analysis. Primary differences between the two applications include the installed power required (80kW$_{electric_net}$ for automotive vs. ~160kW$_{electric_net}$ for a 40' transit bus), desired power plant durability (nominally 5,000 hours lifetime for automotive vs. 25,000 hours lifetime for buses), and annual manufacturing rate (up to 500,000 systems/year for an individual top selling automobile model vs. <1000 systems/year for total transit bus sales in the US).

The capacity to produce fuel cell systems at high manufacturing rates does not yet exist, and significant investments will have to be made in manufacturing development and facilities in order to enable it. Once the investment decisions are made, it will take several years to develop and fabricate the necessary manufacturing facilities. Furthermore, the supply chain will need to develop which requires negotiation between suppliers and system developers, with details rarely made public. For these reasons, the DOE has consciously decided not to analyze supply chain scenarios at this point, instead opting to concentrate its resources on solidifying the tangible core of the analysis, i.e. the manufacturing and materials costs.

The DOE uses these analyses as tools for R&D management and tracking technological progress in terms of cost. Consequently, non-technical variables are held constant to elucidate the effects of the technical variables. For example, the cost of platinum is held at $1,100 per troy ounce to insulate the study from unpredictable and erratic platinum price fluctuations. Sensitivity analyses are conducted to explore the effects of non-technical parameters.

To maximize the benefit of our work to the fuel cell community, Strategic Analysis Inc. (SA) strives to make each analysis as transparent as possible. The transparency of the assumptions and methodology serve to strengthen the validity of the analysis. We hope that these analyses have been and will continue to be valuable tools to the hydrogen and fuel cell R&D community.

Table of Contents

1 Overview

This report is the sixth annual update of a comprehensive automotive fuel cell cost analysis[1] conducted by Strategic Analysis[2] (SA), under contract to the US Department of Energy (DOE). The first report (hereafter called the "2006 cost report") estimated fuel cell system cost for three different technology levels: a "current" system that reflected 2006 technology, a system based on projected 2010 technology, and another system based on projections for 2015. The 2007 update report incorporated technology advances made in 2007 and re-appraised the projections for 2010 and 2015. Based on the earlier report, it consequently repeated the structure and much of the approach and explanatory text. The 2008, 2009, 2010, and 2011 reports followed suit, and this 2012 report[3] is another annual reappraisal of the state of technology and the corresponding costs. In the 2010 report, the "current" technology and the 2010 projected technology merged, leaving only two technology levels to be examined: the current status (now 2012) and the 2015 projection. The 2011 report covered the significant changes to the current (2011) technology status since the 2010 update report. The reader is directed to read the 2010 report[4] and the 2011 update[5] for a detailed summary of the entire system and its components. This 2012 update will cover current status technology updates since the 2011 report, as well as introduce a 2012 bus system analysis considered alongside the automotive system.

In this multi-year project, SA estimates the material and manufacturing costs of complete 80 kWnet direct-hydrogen Proton Exchange Membrane (PEM) fuel cell systems suitable for powering light-duty automobiles and 160 kWnet systems of the same type suitable for powering 40' transit buses. To assess the cost benefits of mass manufacturing, six annual production rates are examined for each automotive technology level: 1,000, 10,000, 30,000, 80,000, 130,000, and 500,000 systems per year. Since total US 40' bus sales are currently ~4,000 vehicles per year[6], only a 1,000 systems/year production rate was considered for cost analysis.

A Design for Manufacturing and Assembly (DFMA) methodology is used to prepare the cost estimates. However, departing from DFMA standard practice, a markup rate to account for the business expenses of general and administrative (G&A), R&D, scrap, and profit, is not currently included in the cost estimates. In other SA cost estimate projects, an additional 10% cost contingency has often been included, though it has not for this study.

---

[1] "Mass Production Cost Estimation for Direct H_2 PEM Fuel Cell Systems for Automotive Applications," Brian D. James & Jeff Kalinoski, Directed Technologies, Inc., October 2007.

[2] This project was contracted with and initiated by Directed Technologies Inc. (DTI). In July 2011, DTI was purchased by Strategic Analysis Inc. (SA) and thus SA has taken over conduct of the project.

[3] For previous analyses, SA was funded directly by the Department of Energy's Energy Efficiency and Renewable Energy Office. For the 2010 and 2011 Annual Update report, SA was funded by the National Renewable Energy Laboratory. For the 2012 Annual update report, SA is funded by Department of Energy's Energy Efficiency and Renewable Energy Office.

[4] "Mass Production Cost Estimation for Direct H_2 PEM Fuel Cell Systems for Automotive Applications: *2010 Update*," Brian D. James, Jeffrey A. Kalinoski & Kevin N. Baum, Directed Technologies, Inc., 30 September 2010.

[5] "Mass Production Cost Estimation for Direct H_2 PEM Fuel Cell Systems for Automotive Applications: 2011 Update," Brian D. James, Kevin N. Baum & Andrew B. Spisak, Strategic Analysis, Inc., 7 September 2012.

[6] Personal communication with Leslie Eudy, National Renewable Energy Laboratory, 25 October 2012.

In general, the system designs do not change with production rate, but material costs, manufacturing methods, and business-operational assumptions do vary. Cost estimation at very low manufacturing rates (below 1,000 systems per year) presents particular challenges. Traditional low-cost mass-manufacturing methods are not cost-effective due to high per-unit setup and tooling costs and less defined, less automated operations are typically employed. For some repeat parts within the fuel cell stack (e.g. the membrane electrode assemblies (MEAs) and bipolar plates), such a large number of pieces are needed for each system that even at low system production rates (1,000/year), hundreds of thousands of individual parts are needed annually. Thus for these parts, mass-manufacturing cost reductions are achieved even at low system production rates. However, other stack components (e.g. end plates and current collectors), and all balance of plant (BOP) equipment (e.g. compressors, hoses and valves), do not benefit from this manufacturing multiplier effect.

The 2012 system reflects the authors' best estimate of current technology and, with only a few exceptions, is not based on proprietary information. Public presentations by fuel cell companies and other researchers along with extensive review of the patent literature are used as the basis for much of the design and fabrication technologies. Consequently, the presented information may lag behind what is being done "behind the curtain" in fuel cell companies. Nonetheless, the current-technology system provides a benchmark against which the impact of future technologies may be compared. Taken together, the analysis of this system provides a good sense of the likely range of costs for mass-produced automotive fuel cell systems and of the dependence of cost on system performance, manufacturing, and business-operational assumptions.

2 Project Approach

The system examined does not reflect the design of any one manufacturer but is a composite of the best elements from a number of designs. The automotive system is normalized to a system output power of 80 kWnet and the bus system to 160 kWnet, although the gross powers for both systems are derived from the parasitic load of the BOP components. The stack efficiency[7] at rated power is set at 55%, to match the DOE target value. Multiplying this by the theoretical open circuit cell voltage (1.229 V) yields a cell voltage of 0.676 V at peak power. Previous iterations of this report had used an assumed oxidant stoichiometry[8] of 1.5-2.5. However, the addition of the ANL curve fit and subsequent parameter optimization has changed these parameters for 2011 and 2012 as will be discussed in Section 5.1.

The main fuel cell subsystems included in this analysis are:

- Fuel cell stacks
- Air loop
- Humidifier and water recovery loop
- High-temperature coolant loop
- Low-temperature coolant loop
- Fuel loop (but not fuel storage)

[7] Stack efficiency is defined as voltage efficiency X H2 utilization = Cell volts/1.229 X 100%.
[8] Air stoichiometry was 2.5 for the 2010 model and dropped to 1.5 for 2011.

- Fuel cell system controller
- Sensors

Some vehicle electrical system components explicitly excluded from the analysis include:

- Main vehicle battery or ultra-capacitor[9]
- Electric traction motor (that drives the vehicle wheels)
- Traction inverter module (TIM) (for control of the traction motor)
- Vehicle frame, body, interior, or comfort related features (e.g., driver's instruments, seats, and windows)

Many of the components not included in this study are significant contributors to the total fuel cell vehicle cost; however their design and cost are not necessarily dependent on the fuel cell configuration or stack operating conditions. Thus, it is our expectation that the fuel cell system defined in this report is applicable to a variety of vehicle body types and drive configurations.

As mentioned above, the costing methodology employed in this study is the Design for Manufacture and Assembly technique (DFMA[10]). The Ford Motor Company has formally adopted the DFMA process as a systematic means for the design and evaluation of cost optimized components and systems. These techniques are powerful and flexible enough to incorporate historical cost data and manufacturing acumen that have been accumulated by Ford since the earliest days of the company. Since fuel cell system production requires some manufacturing processes not normally found in automotive production, the formal DFMA process and SA's manufacturing database are buttressed with budgetary and price quotations from experts and vendors in other fields. It is possible to choose cost-optimized manufacturing processes and component designs and accurately estimate the cost of the resulting products by combining historical knowledge with the technical understanding of the functionality of the fuel cell system and its component parts.

The cost for any component analyzed via DFMA techniques includes direct material cost, manufacturing cost, assembly costs, and markup. Direct material costs are determined from the exact type and mass of material employed in the component. This cost is usually based upon either historical volume prices for the material or vendor price quotations. In the case of materials not widely used at present, the manufacturing process must be analyzed to determine the probable high-volume price for the material. The manufacturing cost is based upon the required features of the part and the time it takes to generate those features in a typical machine of the appropriate type. The cycle time can be combined with the "machine rate," the hourly cost of the machine based upon amortization of capital and operating costs, and the number of parts made per cycle to yield an accurate manufacturing cost per part. The assembly costs are based upon the amount of time to complete the given operation and the cost of either manual labor or of the automatic assembly process train. The piece cost derived in this fashion is quite accurate

[9] Fuel cell automobiles may be either "purebreds" or "hybrids" depending on whether they have battery (or ultracapacitor) electrical energy storage or not. This analysis only addresses the cost of an 80 kW fuel cell power system and does not include the cost of any peak-power augmentation or hybridizing battery.

[10] Boothroyd, G., P. Dewhurst, and W. Knight. "Product Design for Manufacture and Assembly, Second Edition," 2002.

as it is based upon an exact physical manifestation of the part and the technically feasible means of producing it as well as the historically proven cost of operating the appropriate equipment and amortizing its capital cost. Normally (though not in this report), a percentage markup is applied to the material, manufacturing, and assembly cost to account for profit, general and administrative (G&A) costs, research and development (R&D) costs, and scrap costs. This percentage typically varies with production rate to reflect the efficiencies of mass production. It also changes based on the business type and on the amount of value that the manufacturer or assembler adds to the product.

Cost analyses were performed for mass-manufactured systems at six production rates: 1,000, 10,000, 30,000, 80,000, 130,000, and 500,000 systems per year. System designs did not change with production rate, but material costs, manufacturing methods, and business-operational assumptions (such as markup rates) often varied. Fuel cell stack component costs were derived by combining manufacturers' quotes for materials and manufacturing with detailed DFMA-style analysis.

For some components (e.g. the bipolar plates and the coolant and end gaskets), multiple designs or manufacturing approaches were analyzed. The options were carefully compared and contrasted, then examined within the context of the rest of the system. The best choice for each component was included in the 2012 baseline configuration. Because of the interdependency of the various components, the selection or configuration of one component sometimes affects the selection or configuration of another. In order to handle these combinations, the model was designed with switches for each option, and logic was built in that automatically adjusts variables as needed. As such, the reader should not assume that accurate system costs could be calculated by merely substituting the cost of one component for another, using only the data provided in this report. Instead, data provided on various component options should be used primarily to understand the decision process used to select the approach selected for the baseline configurations.

2.1 Bus System

Fuel cell transit buses represent a growing market segment and a logical application of fuel cell technology. Fuel cell transit buses enjoy several advantages over fuel cell automobiles, particularly in the early years, due the availability of centralized refueling, higher bus power levels (which generally are more economical on a $/kW basis), dedicated maintenance and repair teams, high vehicle utilization, (relatively) less cost sensitivity, and the purchasing decision makers are typically local governments or quasi-government agencies whom are often early adopters of environmentally clean technologies.

The transit bus market generally consists of 40' buses (the common "Metro" bus variety) and 30' buses (typically used for Suburban/Commuter[11] to rail station routes). While the 30' buses can be simply truncated versions of 40' buses, they more commonly are based on a lighter and smaller chassis (often school bus frames) than their 40' counterparts. Whereas 40' buses typically have an expected lifetime of 500k to 1M miles, 30' buses generally have a lower expected lifetime, nominally 200k miles.

[11] Commuter buses are typically shorter in overall length (and wheel base) to provide ease of transit through neighborhoods, a tighter turning radius, and more appropriate seating for a lower customer user base.

There are generally three classes of fuel cell bus architecture[12]:

- hybrid electric: which typically utilize full size fuel cells for motive power and batteries for power augmentation;
- battery dominant: which use the battery as the main power source and typically use a relatively small fuel cell system to "trickle charge" the battery and thereby extend battery range;
- plug-in: which operate primarily on the battery while there is charge, and use the fuel cell as a backup power supply or range extender.

In May 2011, the US Department of Energy issued a Request for Information (RFI) seeking input[13] from industry stakeholders and researchers on performance, durability, and cost targets for fuel cell transit buses and their fuel cell power systems. A joint DOE-Department of Transportation (DOT)/Federal Transit Administration (FTA) workshop was held to discuss the responses, and led to DOE publishing fuel cell bus targets for performance and cost as shown in Figure 1. While not explicitly used in this cost analysis, these proposed targets are used as a guideline for defining the bus fuel cell power plant analyzed in the cost study.

The cost analysis in this report is based on the assumption of a 40' transit bus. Power levels for this class of bus vary widely based primarily on terrain/route and environmental loads. Estimates of fuel cell power plant required[14] net power can be as low as 75 kW for a flat route in a mild climate to 180+kW for a hillier urban route in a hot climate. Accessory loads on buses are much higher than on light duty passenger cars. Electric power is needed for climate control (i.e. cabin air conditioning and heating), opening and closing the doors (which also impacts climate control), and lighting loads. In a hot climate, such as Dallas Texas, accessory loads can reach 30-60 kW, although 30-40 kW is more typical[15]. Industry experts[16] note that the trend may be toward slightly lower fuel cell power levels as future buses become more heavily hybridized and make use of high-power-density batteries (particularly lithium chemistries).

The cost analysis in this report is based on a 160 kW_{net} fuel cell bus power plant. This power level is within the approximate range of existing fuel cell bus demonstration projects[17] as exemplified by the 150 kW Ballard fuel cell buses[18] used in Whistler, Canada for the 2010 winter Olympics, and the 120kW UTC power PureMotion fuel cell bus fleets in California[19] and Connecticut. Selection of a 160 kW_{net} power level is also convenient because it is twice the power of the nominal 80kW_{net} systems used for the light duty automotive analysis, thereby easily facilitating comparisons to the use of two auto power plants.

[12] Personal communication with Leslie Eudy, National Renewable Energy Laboratory, 25 October 2012.
[13] "Fuel Cell Transit Buses", R. Ahluwalia, , X. Wang, R. Kumar, Argonne National Laboratory, 31 January 2012.
[14] Personal communication with Larry Long, Ballard Power Systems, September 2012.
[15] Personal communication with Larry Long, Ballard Power Systems, September 2012.
[16] Personal communication with Peter Bach, Ballard Power Systems, October 2012.
[17] "Fuel Cell Transit Buses", R. Ahluwalia, , X. Wang, R. Kumar, Argonne National Laboratory, 31 January 2012.
[18] The Ballard bus power systems are typically referred to by their gross power rating (150kW). They deliver approximately 140kW net.
[19] "SunLine Unveils Hydrogen-Electric Fuel Cell Bus: Partner in Project with AC Transit", article at American Public Transportation Association website, 12 December 2005, http://www.apta.com/passengertransport/Documents/archive_2251.htm

Parameter	Units	2012 Status	Ultimate Target
Bus Lifetime	years/miles	5/100,000 [a]	12/500,000
Power Plant Lifetime[b,c]	hours	12,000	25,000
Bus Availability	%	60	90
Fuel Fills [d]	per day	1	1 (<10 min)
Bus Cost [e]	$	2,000,000	600,000
Power Plant Cost[b, e]	$	700,000	200,000
Road Call Frequency (Bus/Fuel-Cell System)	miles between road calls (MBRC)	2,500/10,000	4,000/20,000
Operating Time	hours per day/days per week	19/7	20/7
Scheduled and Unscheduled Maintenance Cost [f]	$/mile	1.20	0.40
Range	miles	270	300
Fuel Economy	mgde[g]	7	8

a Status represents NREL fuel cell bus evaluation data. New buses are currently projected to have 8 year/300,000 mile lifetime.

b The power plant is defined as the fuel cell system and the battery system. The fuel cell system includes supporting subsystems such as the air, fuel, coolant, and control subsystems. Power electronics, electric drive, and hydrogen storage tanks are excluded.

c According to an appropriate duty cycle.

d Multiple sequential fuel fills should be possible without increase in fill time.

e Cost projected to a production volume of 400 systems per year. This production volume is assumed for analysis purposes only, and does not represent an anticipated level of sales.

f Excludes mid-life overhaul of power plant.

Figure 1: Proposed DOE targets for fuel cell-powered transit buses (From US DOE[20])

The transit bus driving schedule is expected to consist of much more frequent starts and stops, low fractional time at idle power (due to high and continuous climate control loads), and low fractional time at full power compared to light-duty automotive drive cycles[21]. While average bus speeds depend on many factors, representative average bus speeds[22] are 11-12 miles per hour (mph), with the extremes being a New York City type route (~6 mph average) and a commuter style bus route (~23 mph average). No allowance has been made in the cost analysis to reflect the impact of a particular bus driving schedule.

There are approximately 4,000 forty-foot transit buses sold each year in the United States[23]. However, each transit agency typically orders its own line of customized buses. Thus while orders of identical buses may reach 500 vehicles at the high end, sales are typically much lower. Smaller transit agencies

[20] "Fuel Cell Bus Targets", US Department of Energy Fuel Cell Technologies Program Record, Record # 12012, March 2, 2012. http://www.hydrogen.energy.gov/pdfs/12012_fuel_cell_bus_targets.pdf

[21] Such as the Federal Urban Drive Schedule (FUDS), Federal Highway Drive Schedule (FHDS), Combined Urban/Highway Drive Cycle, LA92, or US06.

[22] Personal communication with Leslie Eudy, National Renewable Energy Laboratory, 25 October 2012.

[23] Personal communication with Leslie Eudy, National Renewable Energy Laboratory, 25 October 2012.

sometimes pool their orders to achieve more favorable pricing. Of all bus types[24] in 2011, diesel engine power plants are the most common (63.5%), followed by CNG/LNG/Blends (at 18.6%), and hybrids (electrics or other) (at only 8.8%). Of hybrid electric 40' transit bus power plants, BAE Systems and Alison are the dominant power plant manufacturers. These factors combine to make quite small the expected annual manufacturing output for a particular manufacturer of bus fuel cell power plant. Consequently, 1,000 buses per year is selected as the single annual manufacturing rate to be examined in the cost study. This is considered a fairly high estimate for near-term fuel cell bus sales, however could alternately be viewed on a low estimate if foreign fuel cell bus sales are included.

3 System Schematics and Bills of Materials

System schematics are a useful method of identifying the main components within a system and how they interact. System flow schematics for each of the systems in the current report are shown below. Note that for clarity, only the main system components are identified in the flow schematics. Figure 2 and Figure 3 display the power system diagrams corresponding to the 2011 and 2012 automotive systems. As the analysis has evolved throughout the course of the annual updates, there has been a general trend toward system simplification. This reflects improvements in technology so as not to need as many parasitic supporting systems and facilitates reduced cost. The path to system simplification is likely to continue, and, in the authors' opinion, remains necessary to achieve or surpass cost parity with internal combustion engines.

The authors have conducted annually updated DFMA analysis of automotive fuel cell systems since 2006. Consequently, to better convey how the fuel cell system has evolved with time, key changes in the system schematics are enumerated below for each year's system (beginning in 2008).

The 2008 fuel cell power system was a fairly standard direct-hydrogen pressurized-air fuel cell system configuration. Main features of the 2008 system included:

- 2 separate liquid-cooled fuel cell stacks, plumbed in parallel but connected electrically in series
- A twin-lobe air compressor
- A twin-lobe exhaust air expander
- A water spray humidifier to both humidify and cool the inlet cathode air after compression
- A liquid/gas heat exchanger to condense water in the exhaust stream for recycle to the air humidifier
- A high-temperature coolant loop of water/ethylene glycol to maintain a stack temperature of ~80°C
- An exhaust loop of water/ethylene-glycol mixture to provide cooling for the exhaust air condenser

[24] 2012 Public Transportation Fact Book, American Public Transportation Association (APTA), 63rd Edition September 2012. Accessed February 2013 at http://www.apta.com/resources/statistics/Documents/FactBook/APTA_2012_Fact%20Book.pdf

    - Only 67% of this loop is included in the system cost, because the remainder of its duty is for components outside of the scope of this analysis
- Twin hydrogen ejectors(high-flow and low-flow) to utilize the high pressure (> 300 psi) in the hydrogen storage tanks to re-circulate anode hydrogen

The 2009 system was much simpler than that of 2008, and differed in the following key ways:

- The number of stacks was reduced from 2 to 1
- A centrifugal compressor replaced the twin-lobe compressor
- A centrifugal expander replaced the twin-lobe expander
- A membrane humidifier replaced the water spray humidifier
- The exhaust gas condenser was eliminated (because there was no need to capture liquid water for the water spray humidifier)
- The low-temperature cooling loop was eliminated (because the condenser had been eliminated)
- The high-temperature radiator was slightly smaller (because the peak operating temperature of the stack had been increased and thus there was a larger temperature difference between the coolant and the ambient temperature)

The 2010 technology system reflected both additions and subtractions to the 2009 BOP, though there was a net increase in complexity. This increase is primarily attributed to feedback received from Dr. Rajesh Ahuwalia of Argonne National Laboratory wherein his modeling work identified the need for both a demister and an air precooler, the latter of which requires the re-addition of a low-temperature loop.

The 2010 system configuration differed from the 2009 version in the following key ways:

- The ejector system was reconfigured with the assumption that the fuel storage system (not included in the cost analysis) handles some of the pressure regulation duties:
    - The proportional valve was removed
    - The pressure transducer was removed
    - An over-pressure cut-off (OPCO) valve was added
    - Check valves were added
    - An inline filter for gas purity excursions was added
- A demister was added in order to ensure that no ice formed in the expander
- A new low-temperature cooling loop (different from the one in the 2008 system) was inserted into the system to cool the previously air-cooled CEM and the new air precooler. It also cooled the traction inverter module (TIM), but as this was outside the boundary of the cost analysis, the fraction of the LTL cost proportionate to the TIM's cooling duty (61%) was excluded from the model.
- The high-temperature radiator was once again smaller than the previous year (because the peak operating temperature of the stack had been increased and thus there was a larger temperature difference between the coolant and the ambient temperature).

The 2011 technology system was nearly identical to the 2010 system. The only change to the system diagram from 2010 was the addition of a temperature sensor to the Air Loop.

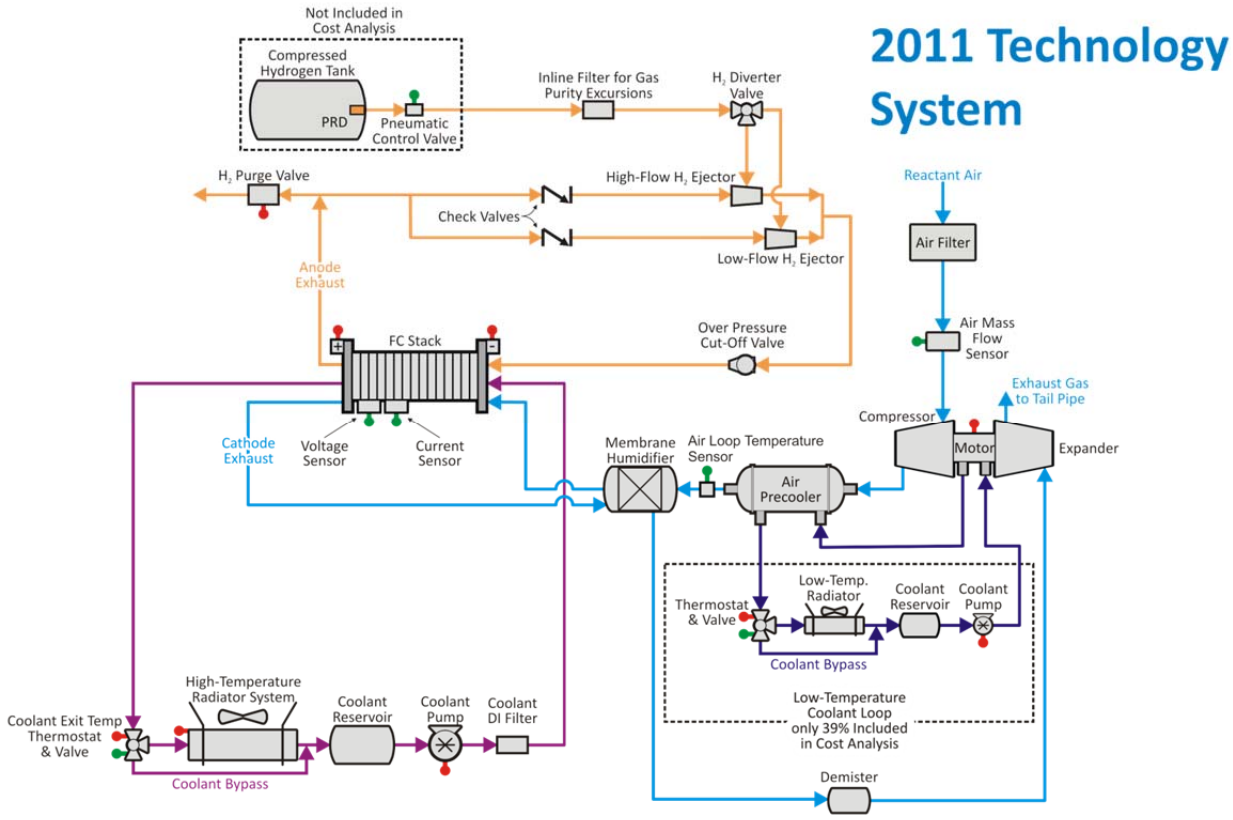

Figure 2: Flow schematic for the 2011 automotive fuel cell system

3.1 2012 Automotive System Schematic

The automotive system schematic for 2012 has not changed from the 2011 system, but is reproduced below for clarity and for comparison to the 2012 bus system schematic.

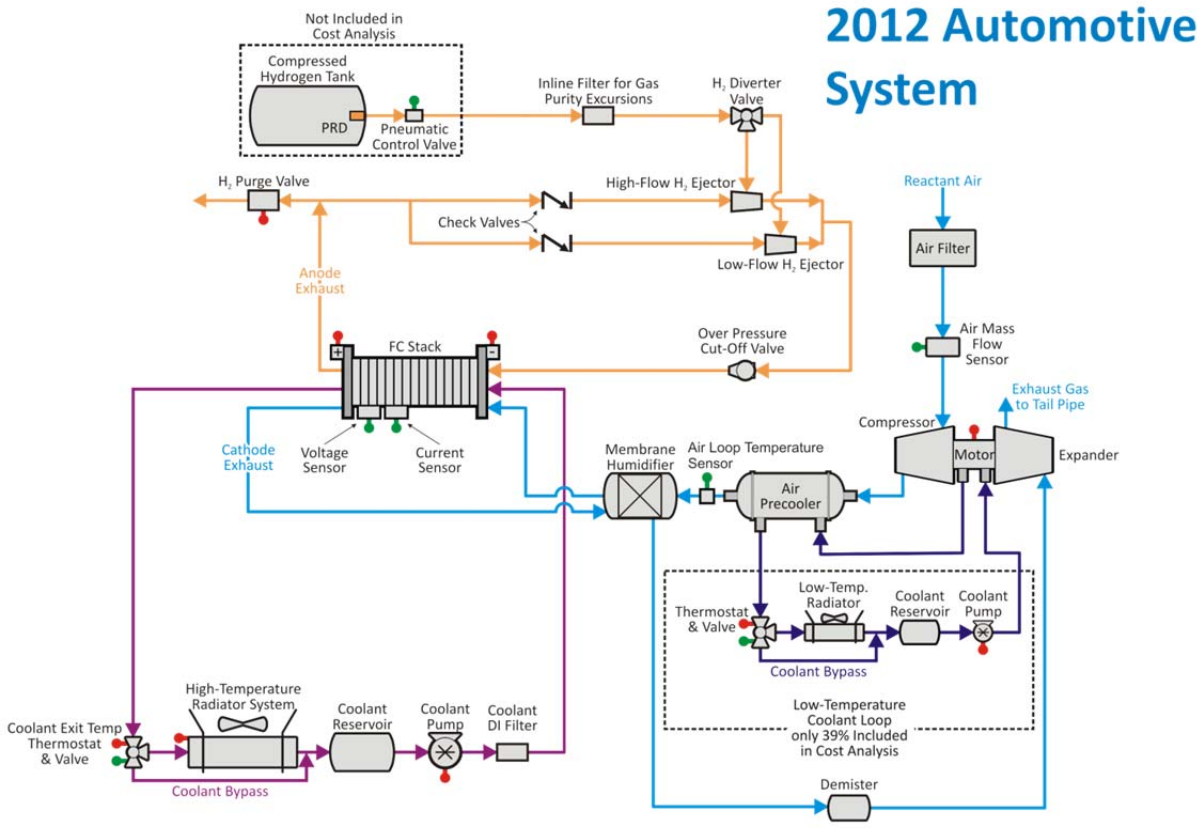

Figure 3: Flow schematic for the 2012 automotive fuel cell system

3.2 2012 Bus System Schematic

The system schematic for the 2012 bus fuel cell power system appears in Figure 4. The power system is directly analogous to the 2012 automotive system with the exception that there are two stacks instead of one, and certain stack-related components are duplicated.

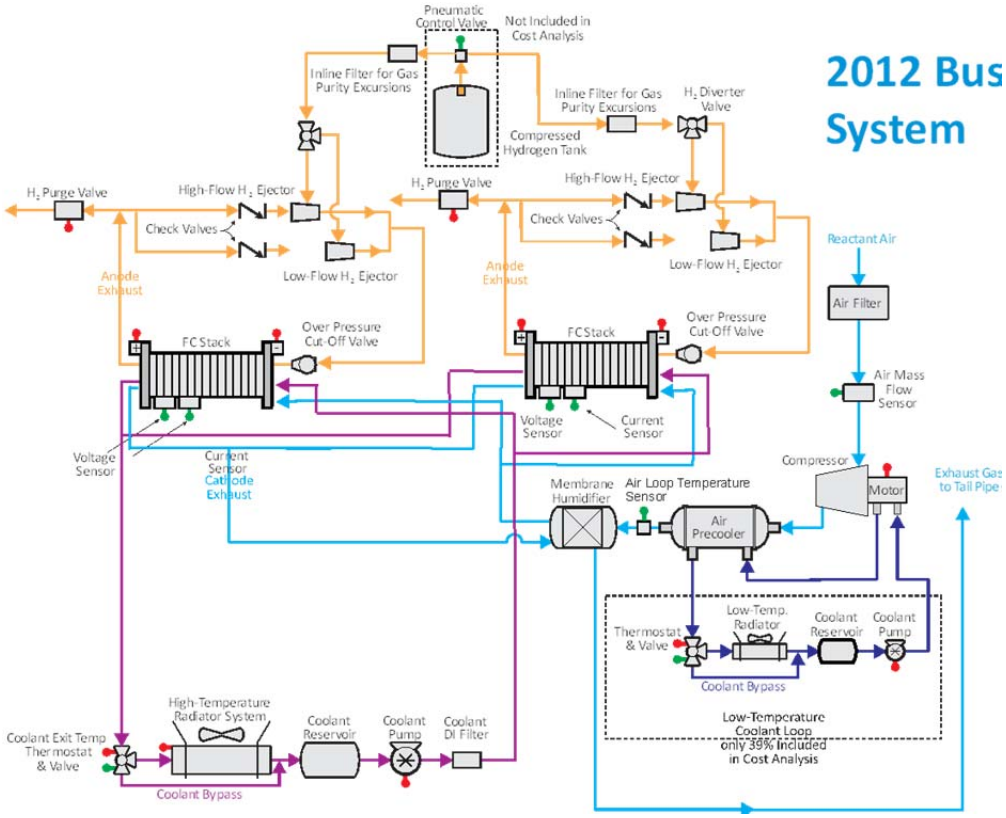

Figure 4: Flow schematic for the 2012 bus fuel cell system

4 System Cost Summaries

Complete fuel cell power systems are configured to allow assembly of comprehensive system Bills of Materials, which in turn allow comprehensive assessments of system cost. Key parameters for the 2012 automotive and bus fuel cell power systems are shown in Figure 5 below, with cost result summaries detailed in subsequent report sections.

	2011 Auto Technology System	2012 Auto Technology System	2012 Bus Technology System
Power Density (mW/cm^2)	1,100	984	716
Total Pt loading ($mgPt/cm^2$)	0.186	0.196	0.4
Net Power (kW_{net})	80	80	160
Gross Power (kW_{gross})	89.25	88.24	177.10
Operating Pressure (atm)	3.00	2.50	1.80
Peak Stack Temp. (°C)	95	87	74
Active Cells	369	369	739
Membrane Material	Nafion on 25-micron ePTFE	Nafion on 25-micron ePTFE	Nafion on 25-micron ePTFE
Radiator/ Cooling System	Aluminum Radiator, Water/Glycol Coolant, DI Filter, Air Precooler	Aluminum Radiator, Water/Glycol Coolant, DI Filter, Air Precooler	Aluminum Radiator, Water/Glycol Coolant, DI Filter, Air Precooler
Bipolar Plates	Stamped SS 316L with TreadStone Coating	Stamped SS 316L with TreadStone Coating	Stamped SS 316L with TreadStone Coating
Air Compression	Centrifugal Compressor, Radial-Inflow Expander	Centrifugal Compressor, Radial-Inflow Expander	Centrifugal Compressor, Without Expander
Gas Diffusion Layers	Carbon Paper Macroporous Layer with Microporous Layer	Carbon Paper Macroporous Layer with Microporous Layer (Ballard Cost)	Carbon Paper Macroporous Layer with Microporous Layer (Ballard Cost)
Catalyst Application	Nanostructured Thin Film (NSTF)	Nanostructured Thin Film (NSTF)	Nanostructured Thin Film (NSTF)
Air Humidification	Tubular Membrane Humidifier	Tubular Membrane Humidifier	Tubular Membrane Humidifier
Hydrogen Humidification	None	None	None
Exhaust Water Recovery	None	None	None
MEA Containment and Gasketing	Injection-Molded LIM Hydrocarbon MEA Frame/Gasket around Hot-Pressed M&E	Screen Printed Seal on MEA Subgaskets, GDL crimpted to CCM	Screen Printed Seal on MEA Subgaskets, GDL crimpted to CCM
Coolant & End Gaskets	Laser Welded (Cooling), Screen-Printed Adhesive Resin (End)	Laser Welded (Cooling), Screen-Printed Adhesive Resin (End)	Laser Welded (Cooling), Screen-Printed Adhesive Resin (End)
Freeze Protection	Drain Water at Shutdown	Drain Water at Shutdown	Drain Water at Shutdown
Hydrogen Sensors	2 for FC System 1 for Passenger Cabin (not in cost estimate) 1 for Fuel System (not in cost estimate)	2 for FC System 1 for Passenger Cabin (not in cost estimate) 1 for Fuel System (not in cost estimate)	2 for FC System 1 for Passenger Cabin (not in cost estimate) 1 for Fuel System (not in cost estimate)
End Plates/ Compression System	Composite Molded End Plates with Compression Bands	Composite Molded End Plates with Compression Bands	Composite Molded End Plates with Compression Bands
Stack Conditioning (hrs)	5	5	5

Figure 5: Summary chart of the 2011 and 2012 automotive systems

4.1 Cost Summary of the 2012 Automotive System

Results of the cost analysis of the 2012 automotive technology system at each of the six annual production rates are shown below. Figure 6 details the cost of the stacks, Figure 7 details the cost of the balance of plant components, and Figure 8 details the cost summation for the system.

	2012 Automotive System					
Annual Production Rate	**1,000**	**10,000**	**30,000**	**80,000**	**130,000**	**500,000**
System Net Electric Power (Output)	80	80	80	80	80	80
System Gross Electric Power (Output)	88.24	88.24	88.24	88.24	88.24	88.24
Bipolar Plates (Stamped)	$1,819.33	$436.67	$411.17	$395.16	$395.55	$392.33
MEAs	$9,082.91	$2,623.29	$1,758.30	$1,415.04	$1,307.39	$1,103.35
Membranes	$3,518.73	$882.16	$495.01	$336.62	$276.84	$171.17
Catalyst Ink & Application (NSTF)	$1,452.68	$816.70	$770.79	$764.76	$763.42	$759.85
GDLs	$2,137.41	$638.84	$359.04	$214.65	$166.39	$82.09
M & E Cutting & Slitting	$487.44	$50.71	$18.36	$8.24	$5.91	$3.15
MEA Gaskets	$1,486.64	$234.87	$115.10	$90.78	$94.83	$87.10
Coolant Gaskets (Laser Welding)	$212.59	$41.52	$28.59	$26.98	$26.60	$26.01
End Gaskets (Screen Printing)	$149.48	$15.04	$5.08	$1.97	$1.25	$0.53
End Plates	$96.65	$33.18	$29.35	$24.93	$22.55	$17.12
Current Collectors	$52.57	$11.40	$7.61	$5.74	$5.16	$4.53
Compression Bands	$10.00	$9.00	$8.00	$6.00	$5.50	$5.00
Stack Housing	$60.50	$10.32	$6.61	$5.51	$4.94	$4.37
Stack Assembly	$76.12	$59.00	$40.69	$34.95	$33.62	$32.06
Stack Conditioning	$170.88	$56.78	$53.87	$47.18	$41.38	$28.06
Total Stack Cost	$11,731.03	$3,296.20	$2,349.26	$1,963.46	$1,843.95	$1,613.36
Total Stack Cost ($/kW$_{net}$)	$146.64	$41.20	$29.37	$24.54	$23.05	$20.17
Total Stack Cost ($/kW$_{gross}$)	$132.94	$37.35	$26.62	$22.25	$20.90	$18.28

Figure 6: Detailed stack cost for the 2012 automotive technology system

	2012 Automotive System					
Annual Production Rate	**1,000**	**10,000**	**30,000**	**80,000**	**130,000**	**500,000**
System Net Electric Power (Output)	80	80	80	80	80	80
System Gross Electric Power (Output)	88.24	88.24	88.24	88.24	88.24	88.24
Air Loop	$1,736.16	$1,039.80	$1,038.41	$897.04	$869.19	$842.01
Humidifier and Water Recovery Loop	$645.60	$226.62	$152.81	$118.09	$107.69	$91.59
High-Temperature Coolant Loop	$537.05	$461.95	$461.76	$405.14	$383.32	$356.58
Low-Temperature Coolant Loop	$96.04	$86.43	$86.32	$80.30	$75.88	$71.33
Fuel Loop	$348.71	$303.32	$293.76	$263.92	$253.63	$240.38
System Controller	$171.07	$150.54	$136.85	$102.64	$95.80	$82.11
Sensors	$1,706.65	$893.00	$893.00	$659.96	$543.45	$225.49
Miscellaneous	$286.39	$166.62	$157.87	$144.25	$139.42	$135.08
Total BOP Cost	$5,527.67		$3,220.79	$2,671.34	$2,468.38	$2,044.57
Total BOP Cost ($/kW$_{net}$)	$69.10		$40.26	$33.39	$30.85	$25.56
Total BOP Cost ($/kW$_{gross}$)	$62.64		$36.50	$30.27	$27.97	$23.17

Figure 7: Detailed balance of plant cost for the 2012 automotive technology system

	2012 Automotive System					
Annual Production Rate	**1,000**	**10,000**	**30,000**	**80,000**	**130,000**	**500,000**
System Net Electric Power (Output)	80	80	80	80	80	80
System Gross Electric Power (Output)	88.24	88.24	88.24	88.24	88.24	88.24
Fuel Cell Stacks	$11,731.03	$3,296.20	$2,349.26	$1,963.46	$1,843.95	$1,613.36
Balance of Plant	$5,527.67	$3,328.28	$3,220.79	$2,671.34	$2,468.38	$2,044.57
System Assembly & Testing	$145.13	$100.62	$98.90	$98.69	$98.24	$98.25
Total System Cost ($)	$17,403.83	$6,725.10	$5,668.96	$4,733.49	$4,410.57	$3,756.18
Total System Cost ($/kW$_{net}$)	$217.55	$84.06	$70.86	$59.17	$55.13	$46.95
Total System Cost ($/kW$_{gross}$)	$197.23	$76.21	$64.24	$53.64	$49.98	$42.57

Figure 8: Detailed system cost for the 2012 automotive technology system

4.2 Cost Summary of the 2012 Bus System

Results of the cost analysis of the 2012 bus technology system at the 1,000 systems per year production rate are shown below. Figure 9 details the cost of the stacks, Figure 10 details the cost of the balance of plant components, and Figure 11 details the cost summation for the system.

	2012 Bus System
Annual Production Rate	**1,000**
System Net Electric Power (Output)	160
System Gross Electric Power (Output)	177.10
Bipolar Plates (Stamped)	$1,141.17
MEAs	
Membranes	$2,595.88
Catalyst Ink & Application (NSTF)	$2,466.74
GDLs	$2,959.34
M & E Cutting & Slitting	$245.32
MEA Gaskets	$799.98
Coolant Gaskets (Laser Welding)	$111.62
End Gaskets (Screen Printing)	$74.80
End Plates	$77.51
Current Collectors	$32.20
Compression Bands	$10.00
Stack Housing	$66.55
Stack Assembly	$73.63
Stack Conditioning	$170.88
Total Stack Cost (single stack)	$10,825.62
Total Stack Cost ($/kW$_{net}$)	$135.32
Total Stack Cost ($/kW$_{gross}$)	$122.25

Figure 9: Detailed stack cost for the 2012 bus technology system

	2012 Bus System
Annual Production Rate	**1,000**
System Net Electric Power (Output)	160
System Gross Electric Power (Output)	177.10
Air Loop	$2,355.14
Humidifier and Water Recovery Loop	$964.62
High-Temperature Coolant Loop	$1,187.73
Low-Temperature Coolant Loop	$142.73
Fuel Loop	$641.99
System Controller	$342.14
Sensors	$2,573.98
Miscellaneous	$498.71
Total BOP Cost	$8,707.03
Total BOP Cost ($/kW$_{net}$)	$54.42
Total BOP Cost ($/kW$_{gross}$)	$49.16

Figure 10: Detailed balance of plant cost for the 2012 bus technology system

	2012 Bus System
Annual Production Rate	**1,000**
System Net Electric Power (Output)	160
System Gross Electric Power (Output)	177.10
Fuel Cell Stacks	$21,651.24
Balance of Plant	$8,707.03
System Assembly & Testing	$152.34
Total System Cost ($)	$30,510.60
Total System Cost ($/kW$_{net}$)	$190.69
Total System Cost ($/kW$_{gross}$)	$172.28

Figure 11: Detailed system cost for the 2012 bus technology system

5 Automotive Power System Changes since the 2011 Report

This report represents the sixth annual update of the 2006 SA fuel cell cost estimate report[25] under contract to the DOE. The 2006 report (dated October 2007) documented cost estimates for fuel cell systems based on projected 2006, 2010, and 2015 technologies. Like the other five updates before it, this annual report updates the previous work to incorporate advances made over the course of 2012. These advances include new technologies, improvements and corrections made in the cost analysis, and alterations of how the systems are likely to develop. This 2012 analysis closely matches the methodology and results formatting of the 2011 analysis[26]. Consequently, the reader is referred to that report for additional description of cost analysis assumptions and manufacturing procedures.

Like the 2011 update, the substantive changes this year revolve around stack components. Argonne National Laboratory (ANL) provided updated 2012 stack polarization modeling results of 3M nanostructured thin film (NSTF) catalyst membrane electrode assemblies (MEA's). These results are used in to re-optimize the stack operating conditions and catalyst loading for the 2012 cost estimation (Section 5.1). Additional changes to the stack components involve updating the stack design and manufacturing methods to involve a handful of new technologies and the most up-to-date feedback from industry. These changes include switching from hot pressing to a crimping roller to be more compatible with NSTF catalyst (Section 5.5.3), changing the MEA gasket design from frame gaskets to thin-film sub-gaskets with screen-printed seals (Section 5.3), and materials cost changes for ionomer (Section 5.2) and the gas diffusion layer (GDL) (Section 5.4).

Noteworthy changes since the 2011 update report and the corresponding effects on system cost are listed in Figure 12 below.

[25] "Mass Production Cost Estimation for Direct H_2 PEM Fuel Cell Systems for Automotive Applications", Brian D. James, Jeff Kalinoski, Directed Technologies Inc., October 2007.
[26] "Mass Production Cost Estimation for Direct H_2 PEM Fuel Cell Systems for Automotive Applications: 2011 Update," Brian D. James, Kevin N. Baum & Andrew B. Spisak, Strategic Analysis, Inc., 7 September 2012.

Change	Reason	Change from previous value	Cost (500k systems/year, $/kW)
Final Value for 2011			***$47.71***
Piping configuration/costing updated and expanded	Response to industry review	$0.76	$48.47
Purge valve upgraded to multi-function model	Response to industry review	$0.34	$48.81
Hot pressing process removed and replaced with crimping roller process prior to cutting and slitting	Hot pressing incompatible with NSTF catalyst deposition, new method required for combining membrane & GDL layers	-$0.05	$48.76
Ionomer cost curve reduction	Ionomer cost curve changed to reflect industry estimated value at high production	-$0.23	$48.53
Pressure, platinum loading, power density, and temperature updated to 2012 ANL optimization values	New release of ANL optimization curves for performance parameters	$1.83	$50.36
Membrane air humidifier design change	Air humidifier changed to tubular design (effect offset by ionomer cost reduction)	$0.25	$50.61
Gaskets changed from frame gaskets to sub-gaskets with screen-printed seals	New manufacturing process modeled in response to industry discussions	-$2.14	$48.47
GDL Analysis Replaced with values from Ballard Analysis	Response to Tech Team review	-$1.52	$46.95
Final Value for 2012		***-$0.76***	***$46.95***

Figure 12. Changes in automotive power system costs since 2011 update

5.1 2012 ANL Polarization Optimization

Argonne National Laboratory updated their modeling results for 2012 to include additional experimental data using 3M nanostructured thin film (NSTF) catalysts. Discussion with Argonne researchers[27] concluded that that the previously-identified preferred air stoichiometry value of 1.5 was unlikely to change with the new data. Furthermore, internal ANL modeling optimization was used to determine the stack operating temperature leading to highest power density. Combining the above factors, and limiting consideration to 0.676 volts/cell, allowed for simplification of the 2012 ANL polarization modeling results to a simple function of two variables: power density and temperature results as a function of pressure and catalyst loading for a fixed air stoichiometry of 1.5. Figure 13 and Figure 14 show the 2012 ANL power density data and optimal stack temperature, respectively. All results assume 0.05mgPt/cm^2 anode catalyst loading. Consistent with the 2011 ANL modeling results, the projections include bipolar plate voltage losses and thus are meant to represent stack-level performance.

[27] Personal communication with Rajesh Ahluwalia, Argonne National Laboratory, July 2012.

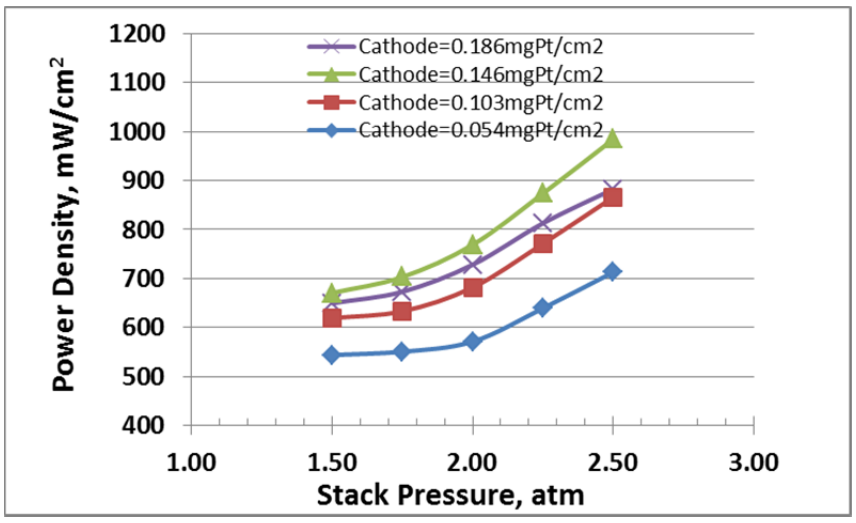

Figure 13: 2012 ANL power density modeling results

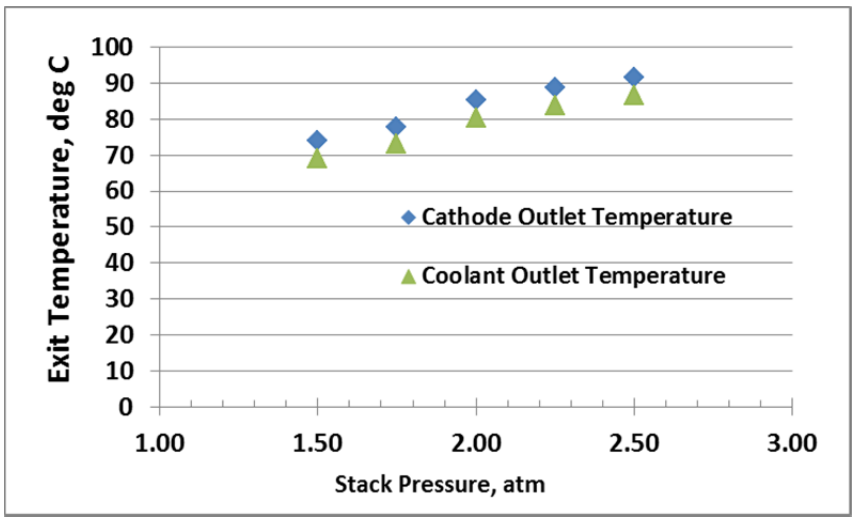

Figure 14: ANL modeling results showing optimal stack temperature as a function of stack pressure

Power density is observed to increase with stack pressure but to peak with a catalyst loading of 0.196mgPt/cm^2 (total) rather than at higher loadings. Discussions with industry researchers[28] suggest that this is due to a catalyst crowding[29] effect. (It is expected that alterations of the length or thickness of the fibrous substrate used within the NSTF system would allow higher catalyst loading without performance decline.)

[28] Personal communication with Mark Debe of 3M and Rajesh Ahluwalia of Argonne National Laboratory, July 2012.

[29] The term "catalyst crowding" is meant to represent the situation where the catalyst layer on the substrate whiskers of the NSTF catalyst layer becomes so thick that it blocks gas flow or otherwise adversely affects performance.

Based on this polarization performance, a system-level cost optimization was conducted to select the operating pressure and catalyst loading that leads to lowest system cost[30]. Figure 15a reveals that system cost decreases with increases in operating pressure at all catalyst loadings. Figure 15b reveals that system cost is minimized at 2.5 atm at a total catalyst loading of 0.196 mgPt/cm^2.

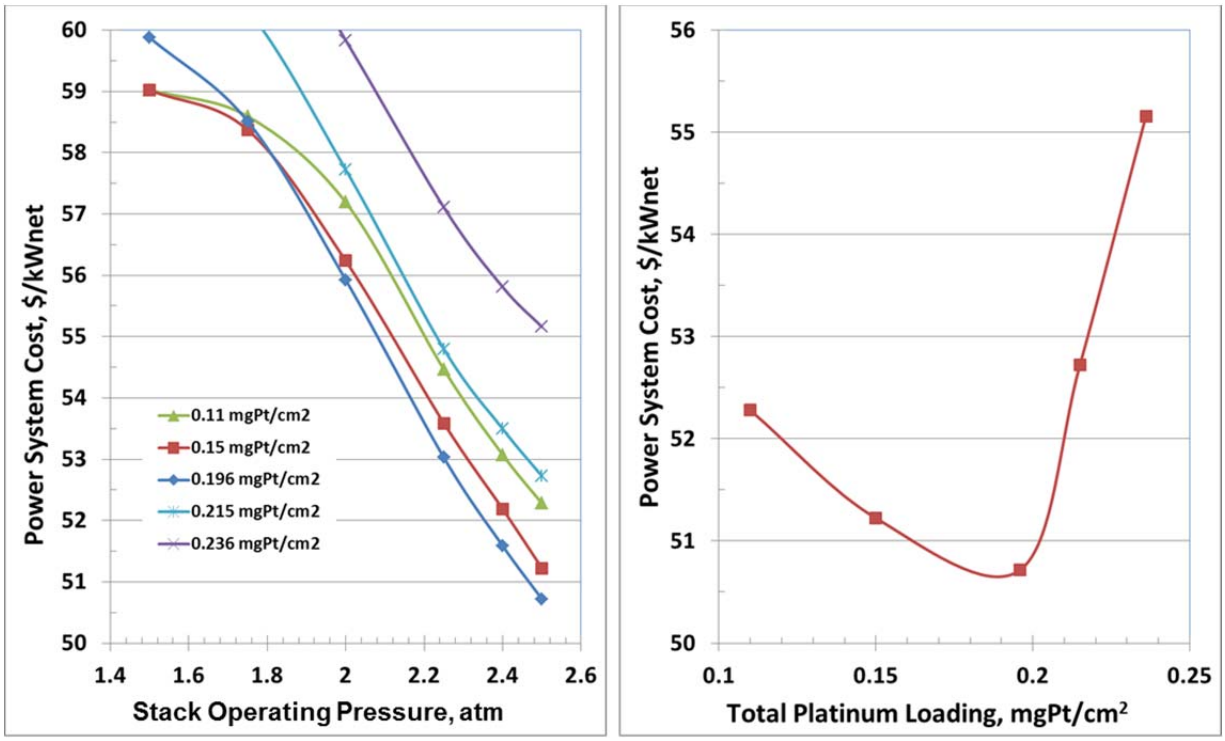

Figure 15: Automotive cost optimization to determine optimal operating pressure and catalyst loading, Left: cost vs. pressure, Right: cost vs. Pt loading

Based on this optimization, the 2012 automotive system beginning-of-life (BOL) stack design conditions at peak power are:

- 0.676 volts/cell
- 1,456 mA/cm2 current density
- 984 mW/cm2 power density
- 2.5 atm stack inlet pressure
- 87°C (outlet coolant temperature)
- 0.196 mgPt/cm2 total catalyst loading

[30] The cost optimization was conducted at a constant 0.676 volts/cell, 1.5 air stoichiometry, and a stack operating temperature optimized by separate AN modeling (and shown in Figure 14).

5.2 Ionomer Cost Reduction

For both the 2011 and 2012 cost analysis, membrane cost was determined by estimating the cost of Nafion ionomer and then conducting a simplified DFMA-style analysis on the processing steps required to transform the ionomer into finished 25.4 micron-thick membrane. A manufacturer's quote for Nafion ionomer (purchase volume dependent) is marked up by 19% to account for markup and a manufacturing process was modeled to simulate the finished ePTFE-supported,hydrated PEM membrane. The cost of ionomer, ePTFE, and manufacturing combine to create a total membrane cost. For the 2012 analysis, the base ionomer manufacturer's cost was modified based on input from the DOE and industry Fuel Cell Technical Team, resulting in a reduced total membrane cost.

SA Cost Model Parameters for Membrane Cost		
500k systems/year, 481 MT ionomer/year	2011 Analysis	2012 Analysis
Ionomer, $/kg	$149/kg $9.41/m^2	$75/kg $4.74/m^2
ePTFE, $/m^2	$8.35 (effective)	$8.35 (effective)
Manufacturing, $/m^2	$5.47	$5.09
Total Membrane Cost, $/m^2	$23.21	$18.18

Figure 16: SA cost model parameters for membrane cost

The new ionomer cost is based upon a 2010 Dow Chemical reference report on high-volume ionomer manufacture[31]. In this report, ionomer material and manufacturing costs are analyzed at extremely high volumes: as high as 6,000 MT/year (where ~500MT/year of material is suitable for 500k vehicles/year). The combination of extremely high production volume and simpler manufacturing process—the industry report models membrane casting rather than application to an ePTFE substrate—results in reported costs much lower than calculated by the SA model. The Fuel Cell Tech Team suggested that the membrane continue to be modeled as an ePTFE-supported membrane and that we adopt the Dow ionomer price at plant sizes more in line with expected annual demand. Consequently for the 2012 analysis, a production-volume-dependent scaling relationship was derived from the Dow report data and used to estimate ionomer price at various fuel cell system annual production rates. This ionomer price curve is shown in Figure 17.

[31] "High Volume Cost Analysis of Perfluorinated Sulfonic Acid Proton Exchange Membranes," Tao Xie, Mark F. Mathias, and Susan L. Bell, General Motors, Inc., May 2010

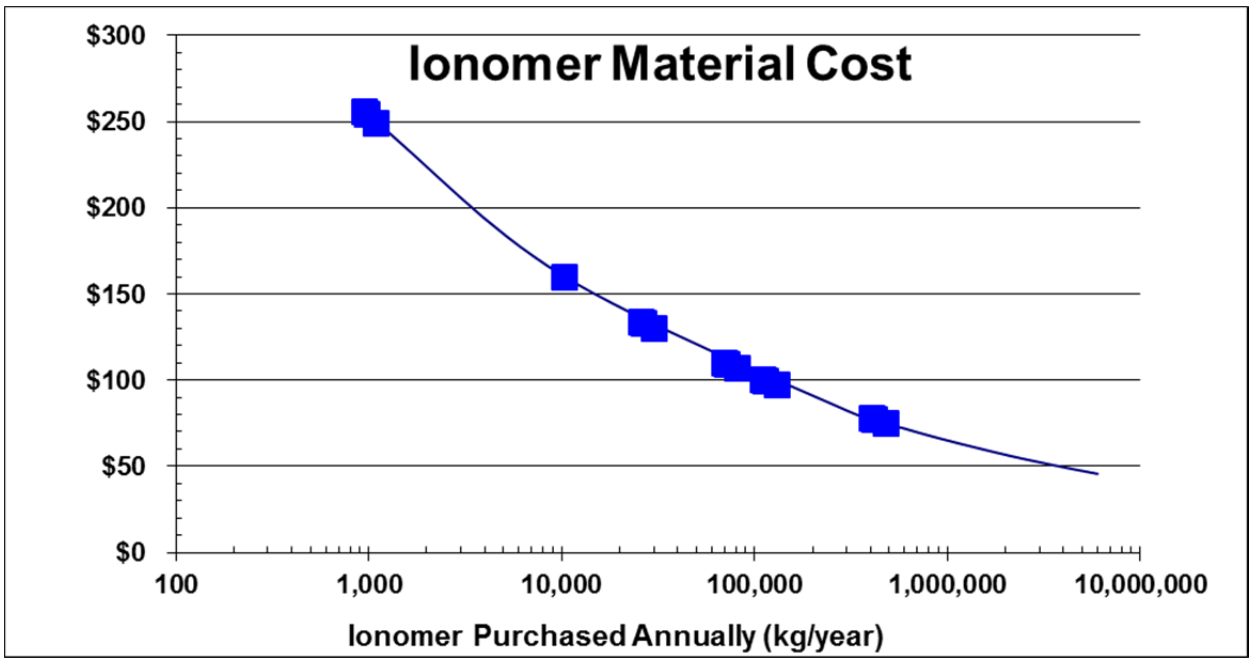

Figure 17: 2012 ionomer material cost curve

5.3 Sub-Gaskets

Systems from prior analysis years used MEA frame gaskets for gas and liquid sealing between the membrane and the bipolar plate. The frame gaskets were insertion-molded around the periphery of the MEA and added substantial cost due to high cycle time and the relatively high cost of custom injection-moldable sealant. Consequently, during the 2012 analysis, an examination was conducted of fuel cell manufacturer processes and patents to identify an alternative lower cost sealing approach. The use of sub-gaskets was identified as a promising alternative.

The sub-gasket sealing approach consists of thin layers of PET gasketing material, judiciously cut into window-frame shapes and laminated to themselves and the periphery of the MEA to form a contiguous and flat sealing surface against the bipolar plate. A thin bead of adhesive sealing material is screen-printed onto the bipolar plates to form a gas- and liquid-tight seal between the bipolar plate and the sub-gasket material. The bipolar plate design has been changed to incorporate a raised surface at the gasket bead location to minimize the use of the gasket material. Screen printing of the gasket bead onto the bipolar plates is a well-understood and demonstrated process. The sub-gasket layers are bonded to the MEA in a roll-to-roll process, shown in Figure 18, based upon a 3M patent application[32]. While the construction is relatively simple in concept, fairly complex machinery is required to handle and attain proper placement and alignment of the thin sub-gasket and MEA layers. This sub-gasket process has four main steps:

1. Formation of a catalyst coated membrane (CCM) web
2. Attachment of membranes to the first half of the sub-gasket ladder web

[32] "Fuel Cell Subassemblies Incorporating Subgasketed Thrifted Membranes," US2011/0151350A1

3. Attachment of the second half of the sub-gasket ladder web to the half sub-gasketed membrane
4. Attach GDLs to sub-gasketed membrane and cut to form individual five-layer MEAs

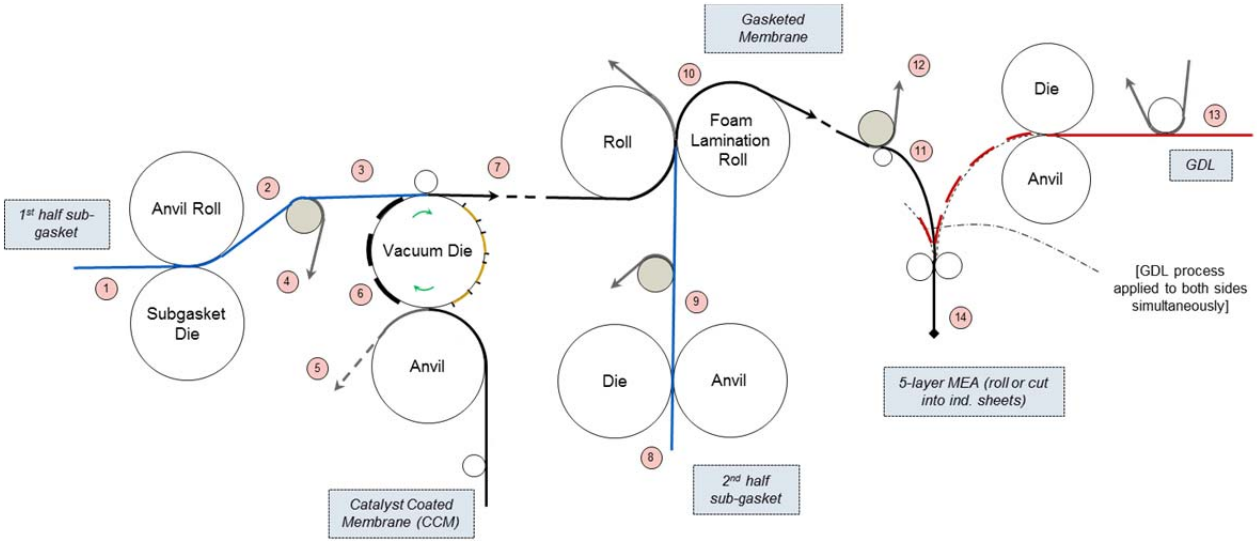

Figure 18: Roll-to-roll subgasket application process

The process uses a proprietary 3M "pressure sensitive adhesive," which is modeled at a notional $20/kg based on high end generic adhesive surrogates. The sub-gasket layer consists of two layers of 0.1mm PET film at $1.67/m^2 based on a high-volume internet price quote. These materials experience significant waste using this process, as the center section of both the sub-gasket layers (corresponding to the fuel cell active area) and the adhesive liner is scrapped. The process capital equipment is based on component analogy to membrane web processing units and is assumed to operate at a line speed of 30m/min with five line workers.

A thin bead of sealing material is screen printed onto the bipolar plates to form a gas and liquid tight seal between the bipolar plate and the sub-gasket material. This process is directly analogous to the screen-printed coolant gaskets analyzed in past cost analyses[33]. The cost of this screen printing step is combined with than of the sub-gasket procedure described above, and presented as a single cost result in Figure 6.

5.4 GDL Cost Reduction

The gas diffusion layer (GDL) costs for 2011 and previous analyses were based upon a price quote for a vendor macroporous layer combined with a DFMA analysis of a microporous layer addition. This resulted in a GDL cost of $11/m^2 at 500k systems/year ($2.54/kWnet).

The new 2012 GDL cost estimate is based on recent DOE-funded research by Ballard Power Systems for cost reduction of a teflonated ready-to-assemble GDL consisting of a non-woven carbon base layer with

[33] The reader is directed to section 4.4.9.3 of the 2010 update of the auto fuel cell cost analysis for a more detailed discussion. "Mass Production Cost Estimation for Direct H_2 PEM Fuel Cell Systems for Automotive Applications: *2010 Update*," Brian D. James, Jeffrey A. Kalinoski & Kevin N. Baum, Directed Technologies, Inc., 30 September 2010.

two microporous layers[34]. The Ballard analysis[35] estimates a cost of $4.45/m^2 at 10M m^2/year (approximately equivalent to 500k systems/year) and a cost of $56/m^2 at less than 100k m^2/year (approximately equivalent to 5k systems/year). Based upon these data points, a learning curve exponent of 0.6952 was derived and used to estimate the GDL cost at intermediate production rates. Figure 19 graphically portrays GDL cost used in the analysis as a function of annual GDL production.

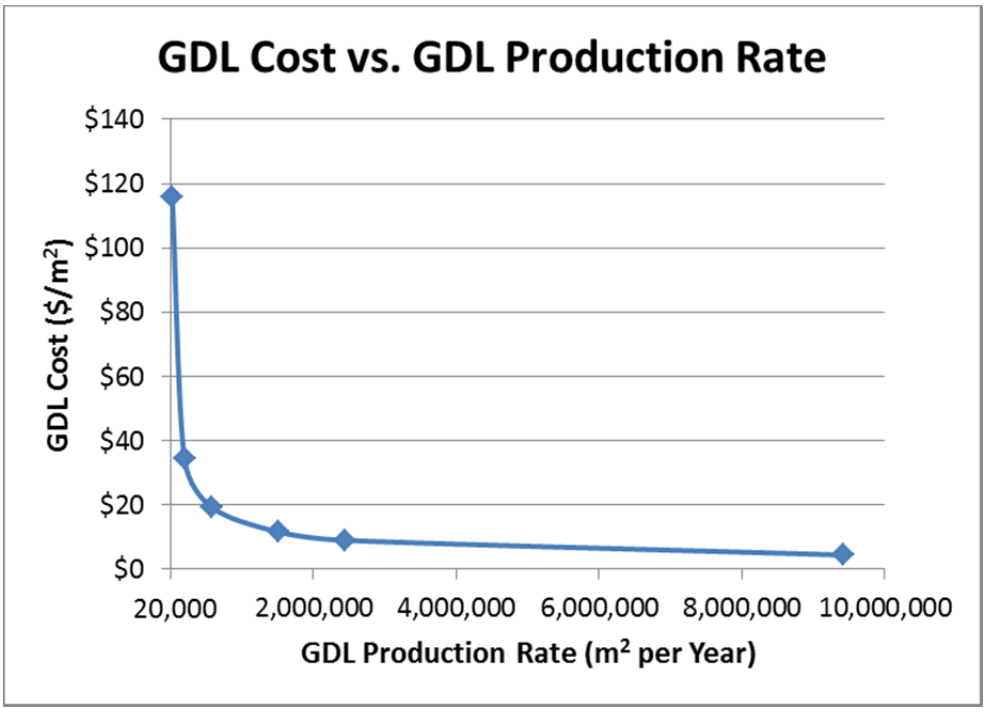

Figure 19: GDL cost as a function of production rate

5.5 Additional Minor Changes

In addition to the above changes, a series of minor improvements was made to the automotive cost analysis. Each is briefly described below.

5.5.1 Piping Configuration Update

Industry feedback provided guidance for a more sophisticated analysis of the piping costs. Previous years' analyses included piping costs based on a certain percentage of calculated base system costs for the high temperature cooling, low temperature cooling, and fuel loop subsystems. The new analysis incorporates a slightly more sophisticated methodology based on the expected type and length of each piping run and the expected number of fittings, pipe bends, and welds. While this yields only a rough approximation of piping cost, achieving a more accurate cost analysis would require a detailed layout of all system components and is beyond the scope of work. Basic assumptions used in the analysis appear below and in Figure 20, with the piping system cost tabulated in Figure 21.

[34] "Reduction in Fabrication Costs of Gas Diffusion Layers," Jason Morgan, Ballard Power Systems, DOE Annual Merit Review, May 2011.
[35] Personal communication with Jason Morgan of Ballard Power Systems, 24 July 2012.

- 5 Bends per meter of pipe ($2.00 per bend)
- 1 Fastener per meter of pipe ($0.10 per fastener)
- 2” Rubber hose for the Air Loop
- 1” Coolant hose for the HT Loop and LT Loop
- 1/2" Schedule 10 stainless steel 316 pipe for the hydrogen loop

Material Costs		
2" Rubber Pipe (Air Loop)	$/m	$23.03
1" Coolant Pipe (HTL and LTL Loops)	$/m	$4.34
1/2" SS 316 Schedule 10 (H^2 Loop)	$/m	$10.76
2" Rubber Pipe Fitting	$/part	$0.75
1" Coolant Hose Fitting	$/part	$0.75
1/2" SS 316 Schedule 10 Fitting	$/part	$3.00
2" Rubber Pipe Fastener	$/part	$0.10
1" Coolant Hose Fastener	$/part	$0.10
1/2" SS 316 Schedule 10 Fastener	$/part	$0.10

Figure 20: Material costs for piping DFMA at 130k systems/year

Air Ducting		
Number of Pipes	7	
Pipe Length	3.3	m
Pipe Cost	$76.00	$/system
Fittings Cost	$9.75	$/system
Fasteners Cost	$0.30	$/system
Air Ducting Total Cost	$86.05	$/system
HTL Piping		
Number of Pipes	7	
Pipe Length	2.35	m
Pipe Cost	$10.20	$/system
Fittings Cost	$10.50	$/system
Fasteners Cost	$0.20	$/system
HTL Piping Total Cost	$20.90	$/system
LTL Piping		
Number of Pipes	7	
Pipe Length	1.9	m
Pipe Cost	$8.25	$/system
Fittings Cost	$10.50	$/system
Fasteners Cost	$0.10	$/system
LTL Piping Total Cost	$18.85	$/system
Hydrogen Piping		
Number of Pipes	8	
Pipe Length	2.45	m
Pipe Cost	$26.36	$/system
Fittings Cost	$45.00	$/system
Fasteners Cost	$0.20	$/system
Bends Cost	$24.00	$/system
Hydrogen Piping Total Cost	$95.56	$/system
Total Pipe Cost	**$120.82**	**$/system**
Total Fittings Cost	**$75.75**	**$/system**
Total Fasteners Cost	**$0.80**	**$/system**
Bends Cost	**$24.00**	**$/system**
Grand Total	**$221.37**	**$/system**

Figure 21: System-by-system piping summary for 130k systems/year

5.5.2 Purge Valve Upgrade

In response to industry feedback, the hydrogen purge valve BOP item has been upgraded to a multi-function model. In previous years' analyses, the purge valve was a standard automotive-style, single-function purge valve quoted at $20 for 30k systems per year which only provided hydrogen gas release as part of the stack purge cycle. The updated purge valve provides additionally for water collection and water purge in addition to the hydrogen purge. The valve design is inspired by Parker Zero Air Loss condensate drains as shown in Figure 22. As Figure 23 indicates, cost is estimated at $63.53 for 30k systems per year based upon a simplified DFMA-style analysis of the materials and assembly cost.

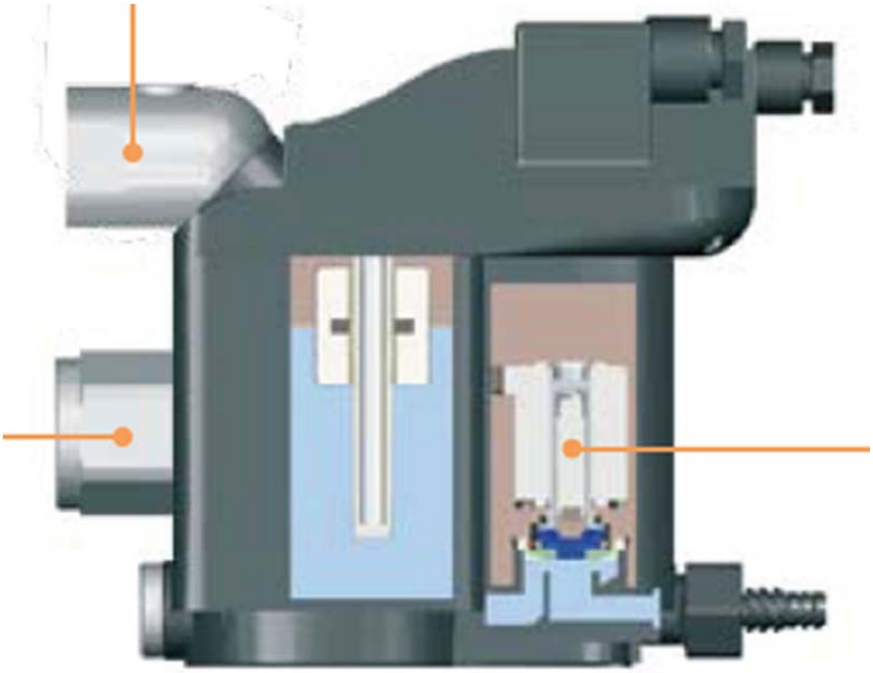

Figure 22: Parker Zero Loss Condensate Drain Diagram[36]

Purge Valve		
Part	**Qty**	**Cost**
plastic housing	1	$10.00
fittings	4	$2.00
solenoid	1	$25.00
float	1	$5.00
Material Total	**1**	**$48.00**
Assembly		
Time	min	3.00
Labor	$/hr	$44.00
Labor Total		$2.20
Markup		
15% markup		$7.53
10% Miscellaneous		$5.77
Grand Total		**$63.50**

Figure 23: Purge valve cost basis for 30k parts/year

[36] Bulletin 1300-600/USA Parker Zero Air Loss Condensate Drains For Compressed Air and Gas, Feb 2007.

5.5.3 Crimping Roller Replacing Hot Pressing

Industry feedback[37] confirmed that the previous modeled procedure of hot pressing the membrane and GDL to bond the parts was incompatible with the NSTF catalyst layer[38]. Bonding of the three layers of the MEA (the catalyst-coated membrane plus GDL on either side) is desirable for proper alignment of the parts as well as ease of handling during the MEA gasketing process. Consequently for the 2012 cost analysis, the layers of the MEA are crimped together periodically along the edges as part of the cutting and slitting process, to an extent sufficient to hold the assembly together until the sub-gasketing process is complete. Cost of the operation is very low, as it merely requires an extra roller assembly in the cutting and slitting process line.

5.5.4 Membrane Air Humidifier Design Change

The cathode membrane humidifier design for 2012 reflects a modified version of the tubular air humidifiers from previous years' analysis. This humidifier is based upon a PermaPure tubular membrane humidifier, resized slightly and incorporating the lower-cost ionomer (as described in section 5.2). Future analyses are intended to include a new plate-frame humidifier modeled after products by Gore, but that analysis was not completed in time for inclusion in the 2012 analysis. Since plate-frame humidifiers may more readily utilize a membrane support layer, thinner membranes are more feasible than in tubular membrane systems. Water transport is enhanced by a thin membrane, thus plate-frame humidifiers are expected to have lower membrane area and a lower overall volume than tubular humidifier designs. As shown in Figure 24, modeling supports this general observation and confirms that a planar humidifier system with 25 micron membrane thickness is expected to require substantially less membrane area than comparable tubular systems. Thus, while the 2012 cost analysis is based on the larger area tubular humidifier, a size reduction, and potentially cost reduction, is expected next year when the switch to a plate-frame humidifier is made.

[37] Personal communication with Mark Debe of 3M, November 2011.

[38] Previous cost analysis postulated bonding of the GDL and catalyst coated membrane through a hot pressing procedure since the ionomer within the catalyst ink composition could serve as a bonding agent for the GDL. However, there is no ionomer in the NSTF catalyst layer and thus hot pressing would not be effective for NSTF MEA's.

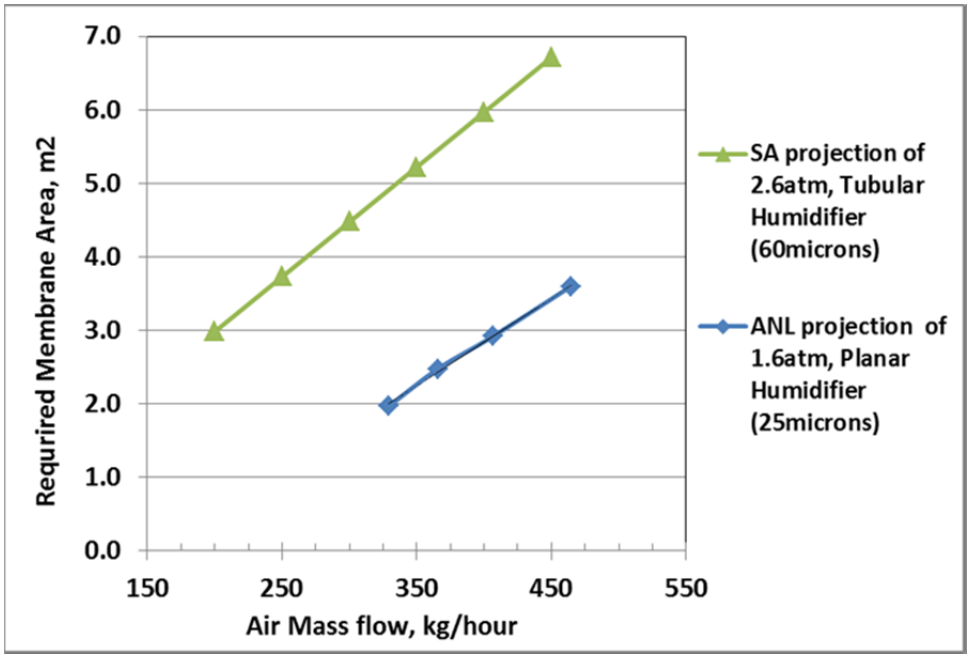

Figure 24: SA vs ANL membrane area projections for tubular and planar humidifier designs

6 Bus Fuel Cell Power System

In addition to the annual cost updated of the automotive fuel cell power system, a transit bus fuel cell power system was analyzed for the first time as part of the 2012 cost report. The bus power system is based substantially upon the 2012 automotive technology system, including all of the above listed changes from the 2011 technology system. The automotive and bus power plants are very similar in operation with key difference consisting primarily of power level, operating pressure, and catalyst loading. Section 6.1 below details the key differences between auto and bus power systems. If no difference is documented in this section, then details of material selection, manufacturing processes, and system design are assumed not to differ from that of the automotive system.

6.1 Bus Power System Overview and Comparison with Automotive Power System

Figure 25 below is a basic comparison summary of the 2012 auto and bus systems. As shown, most stack mechanical construction and system design features are identical between the bus and automotive power plants. Primary system differences include:

- Use of two ~90kW$_{gross}$ fuel cell stacks to achieve a net system power of 160kW$_{net}$ (instead of one ~90kW$_{net}$ stack for an 80kW$_{net}$ power level as used in the automotive system)
- Higher cell platinum loading (0.4mgPt/cm^2 instead of 0.196 mgPt/cm^2 as used in the automotive system)
- Differences in cell active area and number of active cells per stack
- Higher system voltage (reflecting two stacks electrically in series and the desire to keep current below 400 amps)

- Operation at 1.8 atm (instead of 2.5 atm as used in the automotive system)
- Use of a twin lobe air compressor (based on an Eaton design) without an exhaust gas expander (instead of a centrifugal-compressor/radial-inflow-expander based on a Honeywell design as used in the automotive system)
- Reduced stack operating temperature (74°C instead of 87°C as used in the automotive system)
- Increased size in balance of plant components to reflect higher system gross power

	2012 Auto Technology System	2012 Bus Technology System
Power Density (mW/cm^2)	984	716
Total Pt loading ($mgPt/cm^2$)	0.196	0.4
Net Power (kW_{net})	80	160
Gross Power (kW_{gross})	88.24	177.10
Operating Pressure (atm)	2.50	1.80
Peak Stack Temp. (°C)	87	74
Active Cells	369	739
Membrane Material	Nafion on 25-micron ePTFE	Nafion on 25-micron ePTFE
Radiator/ Cooling System	Aluminum Radiator, Water/Glycol Coolant, DI Filter, Air Precooler	Aluminum Radiator, Water/Glycol Coolant, DI Filter, Air Precooler
Bipolar Plates	Stamped SS 316L with TreadStone Coating	Stamped SS 316L with TreadStone Coating
Air Compression	Centrifugal Compressor, Radial-Inflow Expander	Centrifugal Compressor, Without Expander
Gas Diffusion Layers	Carbon Paper Macroporous Layer with Microporous Layer (Ballard Cost)	Carbon Paper Macroporous Layer with Microporous Layer (Ballard Cost)
Catalyst Application	Nanostructured Thin Film (NSTF)	Nanostructured Thin Film (NSTF)
Air Humidification	Tubular Membrane Humidifier	Tubular Membrane Humidifier
Hydrogen Humidification	None	None
Exhaust Water Recovery	None	None
MEA Containment and Gasketing	Screen Printed Seal on MEA Subgaskets, GDL crimpted to CCM	Screen Printed Seal on MEA Subgaskets, GDL crimpted to CCM
Coolant & End Gaskets	Laser Welded (Cooling), Screen-Printed Adhesive Resin (End)	Laser Welded (Cooling), Screen-Printed Adhesive Resin (End)
Freeze Protection	Drain Water at Shutdown	Drain Water at Shutdown
Hydrogen Sensors	2 for FC System 1 for Passenger Cabin (not in cost estimate) 1 for Fuel System (not in cost estimate)	2 for FC System 1 for Passenger Cabin (not in cost estimate) 1 for Fuel System (not in cost estimate)
End Plates/ Compression System	Composite Molded End Plates with Compression Bands	Composite Molded End Plates with Compression Bands
Stack Conditioning (hrs)	5	5

Figure 25: Comparison table between 2012 auto and 2012 bus technology systems

6.2 Bus System Performance Parameters

The bus and automotive power systems function in nearly identical fashion but have different power levels, flow rates, and pressure levels. The following sections describe the sizing methodology and values for key parameters of the bus power system.

6.2.1 Power Level

To provide sufficient power, two 80 kW_{net} stacks are used in parallel, for a total net electrical power of 160 kW. This number was chosen as an intermediate point in existing bus FC power systems, which nominally range from 140 kW_{net} to 190 kW_{net} electrical. Modeling a system which is an even multiple of 80 kW has the additional advantage of allowing a comparison between a dedicated bus system and a pair of automotive systems.

6.2.2 Polarization Performance Basis

Stack performance within the bus systems is based on Argonne National Laboratory modeling of 3M nanostructured thin film catalyst membrane electrode assembly (MEA) performance. The polarization curve model used for the bus stacks is the same as used for the automotive system with modification for different operating conditions and catalyst loading (as discussed below). As understood by the authors, the two main bus fuel cell power plant suppliers, Ballard Power Systems and UTC Power, use the same stack construction and MEA composition within their bus power system stacks as they do for their light-duty vehicle stacks. Consequently, the same is assumed for this report with the exception of catalyst loading.

Thus the 2012 bus power system beginning-of-life (BOL) stack design conditions at peak power are:

- 0.676 volts/cell
- 1,060 mA/cm2 current density
- 716 mW/cm2 power density
- 1.8 atm
- 74°C (outlet coolant temperature)
- 1.5 air stochiometry
- 0.4 mgPt/cm2 total catalyst loading (see section 6.2.3)

Discussions with Ballard[39] regarding their latest generation[40] (HD7) fuel cell stacks suggests an anticipated bus application design peak power operating point of ~0.69 volts/cell at ~1,100 mA/cm^2 yielding a power density of $759mW/cm^2$ at a stack pressure of 1.8 atm and an ~$0.4mgPt/cm^2$ total catalyst loading. This operating point is very close to the selected 2012 bus design point and is thus viewed as validation of the parameter selection.

[39] Personal communication, Peter Bach, Ballard Power Systems, October 2012.

[40] Ballard FCvelocity HD6 stacks are currently used in Ballard bus fleets. The HD7 stack is the next generation stack, has been extensively tested at Ballard, and is expected to be used in both automotive and bus vehicle power systems next year.

As seen in Figure 26, the selected power density is noted to be significantly lower than the design point chosen for the automotive systems (716 vs. 983mW/cm^2) and consequently results in a correspondingly larger bus fuel cell stack.

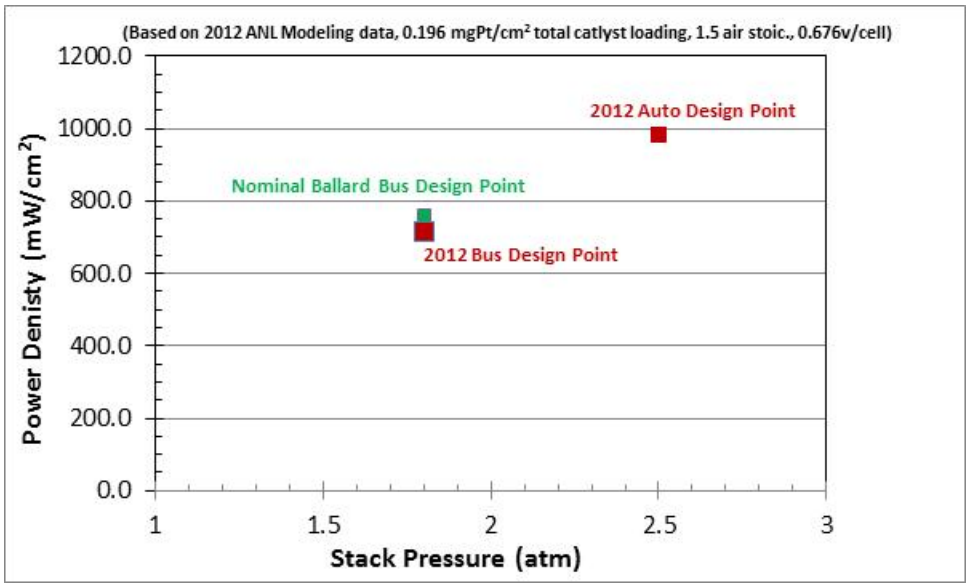

Figure 26: 2012 Bus peak power design point

6.2.3 Catalyst Loading

Catalyst loading is a key driver of system cost and significant effort on the part of fuel cell suppliers has gone towards its reduction. In general, bus applications are less cost-sensitive and have longer lifetime requirements than automotive systems. Consequently, bus fuel cell stacks are more likely to have high catalyst loading since there is a general correlation between platinum loading and stack durability[41]. Examination of the 3M NSTF cell performance as represented by ANL modeling results and through discussion with 3M researchers reveals that increases in catalyst loading past ~0.2mgPt/cm^2 result in declining polarization performance due to a catalyst crowding[42] effect. It is expected that alterations of the length or thickness of the fibrous substrate used within the NSTF system would allow higher catalyst loading without performance decline. Consequently, for the bus application, we model MEA performance as if it corresponds to the 0.196mgPt/cm^2 loading (the same loading used in the automotive system) but attribute a loading of 0.4mgPt/cm^2 for cost computation. This is meant to represent the performance of a bus application NSTF system that has the thin film catalyst layer optimized for both high polarization performance and higher catalyst loading (for durability). This level of catalyst loading is also consistent with the levels used in Ballard fuel cell stacks.

[41] Many factors affect stack lifetime and degradation rate. But to the extent that degradation is caused by platinum catalyst poisoning, reduction in surface area, and/or reduced utilization, high catalyst loading tends to correlate with longer lifetime.

[42] The term “catalyst crowding” is meant to represent the situation where the catalyst layer on the substrate whiskers of the NSTF catalyst layer becomes so thick that it blocks gas flow or otherwise adversely affects performance.

6.2.4 Operating Pressure

As previously stated, the two main fuel cell bus power plant developers are Ballard Power Systems and UTC Power. Recent Ballard buses, using their FCvelocity HD6 fuel cell stacks, typically operating at a stack pressure of ~1.8 atm (at rated power) and do not employ an exhaust gas expander. Recent UTC Power fuel cell bus power plants, using their porous carbon bipolar plates, typically operate near ambient pressure. The UTC Power porous carbon plates allow water management within the cell (both humidification and product water removal) and are a key element of their ability to achieve high polarization performance at low pressure. The porous carbon bipolar plate construction has not been cost-modeled under this effort and it would be inappropriate to postulate the combination of stamped metal bipolar plate construction with performance of NSTF catalyst MEA at near ambient pressure[43]. Consequently, ambient pressure operation is not selected for bus application cost modeling at this time, although it could be considered in future analysis tasks.

A stack pressure of 1.8 atm is selected as the bus system baseline operating stack pressure at rated power to reflect the typical operating conditions used by Ballard. An exhaust gas expander is not used as there is a limited power available from the expansion of gas at this moderate pressure. This operating point of 1.8 atm without expander is in contrast to the optimized automotive system operating conditions of 2.5 atm with expander. To further explore the issue of operating pressure, a sensitivity analysis was conducted. Results are shown report section 10.3.

6.2.5 Stack Operating Temperature

As in the automotive analysis, the design stack temperature[44] at rated (peak) power is determined by ANL modeling which holistically assesses MEA performance, heat generation, and water management within the stack. Stack temperature correlates with operating pressure, and stack temperature at rated power is determined to be 74°C for 1.8 atm. This is a significant reduction from the 87°C temperature of the automotive system at 2.5 atm.

It is noted that Ballard reports their fuel cell bus stack temperatures at only 60°C. The reasons for this are several-fold. First, the system may not typically operate at rated power for long enough times for stack temperature to rise to its nominal value. This is particularly true for a bus power plant for which, depending on the bus route, maximum power may be demanded only a low fraction of the time. Second, various stack and membrane failure mode mechanisms are associated with high temperature. Thus it may desirable to deliberately limit stack peak temperature as a means to achieving the stack lifetime goal of >12,000 hours (this is less of a concern for auto applications with lower lifetime requirements). Thirdly, higher stack temperature reduces the size of the heat rejection temperature since it increases the temperature difference with the ambient air. For an automobile, volume and frontal area are at a premium under the hood. Minimizing the size of the radiator is important for the auto application but is less important for the bus application where radiators may be placed on the roof.

[43] This combination is theoretically possible but experimental data is not readily available nor, to the author's knowledge, have NSTF catalyst MEA parameters been optimized for ambient pressure operation.

[44] For modeling purposes, stack operating temperature is defined as the stack exit coolant temperature. Modeling suggests approximately a 10°C temperature difference between coolant inlet and outlet temperatures and the cathode exhaust temperature to be approximately 5°C higher than coolant exit temperature.

Thus, there are several good reasons—and fewer disadvantages—in selecting a low operating temperature for the bus compared to the auto application.

6.2.6 Cell Active Area and System Voltage

Because the system consists of two stacks electrically in series, system voltage has been set to 500V at design conditions[45]. This bus voltage represents a doubling relative to the automotive system and is necessary to maintain the total electrical current below 400 amps. These values are broadly consistent with the Ballard fuel cell bus voltage range[46] of 465 to 730. Specific cell and system parameters are detailed in Figure 27 for beginning-of-life (BOL) conditions.

Parameter	Value
Cell Voltage (BOL at rated power)	0.676 V/cell
System Voltage (BOL at rated power)	500 V
Number of Stacks	2
Active Cells per Stack	370
Total Cells per System	740
Active Area per Cell	335 cm^2
Stack Gross Power at Rated Power Conditions (BOL)	177 kW

Figure 27: Bus stack parameters

6.3 Air Compression System

The air compression system for the automotive power system is based on a Honeywell-designed centrifugal air compressor mated to a radial inflow exhaust gas expander and a 165,000 rpm permanent magnet motor. However, that compressor-expander-motor (CEM) unit is not used for the bus system. Rather, an Eaton-style twin vortex, Roots-type air compressor such as that currently used in Ballard fuel cell buses is postulated for the cost analysis. A complete DFMA analysis of the Eaton-style air compressor has not been conducted but is planned for future analysis. However, it is expected that an Eaton-style air compressor will have a cost similar to that of a comparable air flow and pressure ratio centrifugal compressor unit. Consequently the DFMA cost of a centrifugal compressor[47] is used as a

[45] For purposed of the system cost analysis, design conditions correlate to rated maximum power at beginning of life.

[46] Ballard FCvelocity-HD6 Spec Sheet. http://www.ballard.com/fuel-cell-products/fc-velocity-hd6.aspx Accessed 9 October 2012.

[47] The 2011 automotive fuel cell analysis conducted by the authors included scaling factors for high speed centrifugal air compressors with integrated permanent magnet motors and controllers, both with and without

surrogate until the Eaton-style air compressor DFMA analysis is available. The bus air compressor unit (including motor and motor controller) is estimated at $1985 at 1,000 units per year. The baseline compressor is modeled on Eaton's R340 supercharger which is in Eaton's Twin Vortices Series (TVS). It is a Roots-type supercharger featuring four lobe rotors, high-flow inlet and outlet ports, and the capability to achieve high efficiency over a wide air flow range. The isentropic efficiency map of the R340 unit is shown in Figure 28. The compressor is mechanically mated to a 24,000 rpm (max) high efficiency brushless motor as shown in Figure 29. Intermeshing of the counter-rotating vortices is shown in Figure 30.

The reader is referred to report section 10.3 which describes a sensitivity study conducted over a range of stack operating pressures. In that sensitivity study, the baseline Eaton compressor is not used. Rather a Honeywell-style compressor-expander-motor (CEM) unit, analogous to that used in the automotive power system, is postulated since a series of compressors and expander units at various compression ratios are needed for the analysis. The previous full-DFMA analysis of the Honeywell-style CEM provides a convenient mechanism for the sensitivity study.

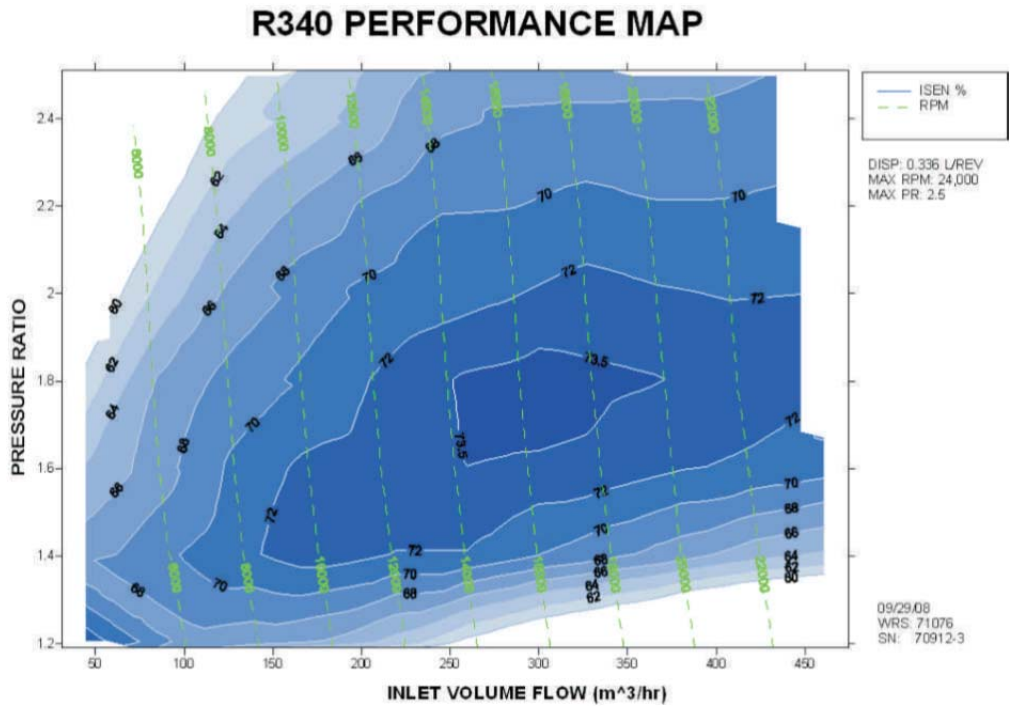

Figure 28: Isentropic efficiency map of the Eaton R340 supercharger

exhaust gas expanders. Thus, to estimate the cost of the bus air blower at 1,000 units/year, the automotive compressor was scaled for air mass flow, pressure ratio, and removal of the expander.

Figure 29: Exterior view of the Eaton R340 supercharger

Figure 30: Interior view of the R340 supercharger vortices

While the Eaton R340 has a peak compression ratio of ~2.5, peak efficiency occurs around a compression ratio of 1.8. While the compressor could be resized to achieve peak efficiency at any targeted air flow, often called the "sweet spot", the R340 unit happens to be very well-sized for the bus fuel cell application[48]. Details of the baseline compressor appear in Figure 31.

[48] This is not coincidental, as Eaton has worked for multiple years to develop cathode air blowers/compressors for fuel cell applications.

Parameter	Value
Compressor Type	Roots (twin vortices)
Compression Ratio at Design Point	1.8
Air Flow Rate at Design Point	463 kg/hour (129 g/s)
Compression Efficiency[49] at Design Point	73.5%
Expander Type	Not used
Combined Motor and Motor Controller Efficiency[50]	85%

Figure 31: Details of the baseline bus air compressor

6.4 Bus System Balance of Plant Components

To accommodate the increased flows and power level of a two-stack 160 kW_{net} system, many balance of plant (BOP) components had to be revised. In some cases, the previous automotive DFMA-style analysis of the balance of plant component automatically adjusted in response to the system design change. In other cases, new quotes were obtained, part scaling was included, or individual parts were increased in number (e.g. some parts are used on each of the two stacks). The changes to BOP components to reflect a bus system are summarized in Figure 32.

Balance of Plant Item	Bus System Change
CEM & Motor Controller	DFMA analysis scaled to new flow and pressure ratio parameters, but switched to design without Expander
Air Mass Flow Sensor	New quote obtained for higher mass flow of bus system
Air Temperature Sensor	No change
Air Filter & Housing	New quote obtained for higher mass flow of bus system
Air Ducting	Piping and tubing diameters increased by a factor of 1.5 to adjust for higher mass flow of bus system
Air Precooler	DFMA analysis scaled to new mass flow and temperature parameters.
Demister	Area size scaled by ratio of bus to automotive air flows
Membrane Air Humidifier	DFMA analysis scaled to new gas mass flow and temperature parameters
HTL Coolant Reservoir	New quote obtained for larger expected coolant liquid volume of bus system
HTL Coolant Pump	New quote obtained for larger expected coolant flow of bus system
HTL Coolant DI Filter	Size scaled by factor of 2 to correspond to higher expected coolant flow rates of bus system
HTL Thermostat & Valve	New quote obtained for larger flow rate and pipe diameter of bus system
HTL Radiator	DFMA analysis scaled to new heat rejection and temperature parameters of bus system
HTL Radiator Fan	New quote obtained corresponding to larger fan diameter and air flow rate parameters of bus system

[49] Compression efficiency is defined as isentropic efficiency.
[50] Combined efficiency is defined as the product of motor efficiency and motor controller efficiency.

HTL Coolant piping	Piping and tubing diameters increased by a factor of 1.5 to adjust for higher coolant flow of bus system
LTL Coolant Reservoir	New quote obtained for larger expected coolant liquid volume of bus system
LTL Coolant Pump	New quote obtained for larger expected coolant flow of bus system
LTL Thermostat & Valve	New quote obtained for larger flow rate and pipe diameter of bus system
LTL Radiator	DFMA analysis scaled to new heat rejection and temperature parameters of bus system
LTL Radiator Fan	New quote obtained corresponding to larger fan diameter and air flow rate parameters of bus system
LTL Coolant Piping	Piping and tubing diameters increased by a factor of 1.5 to adjust for higher coolant flow of bus system
Inline Filter for Gas Purity Excursions	Size scaled by factor of 2 to correlate to increased hydrogen flow rate of bus system
Flow Diverter Valve	Quantity doubled to reflect use of two stacks in bus system
Over-Pressure Cut-Off Valve	Quantity doubled to reflect use of two stacks in bus system
Hydrogen High-Flow Ejector	Quantity doubled to reflect use of two stacks in bus system
Hydrogen Low-Flow Ejector	Quantity doubled to reflect use of two stacks in bus system
Check Valves	Quantity doubled to reflect use of two stacks in bus system
Hydrogen Purge Valve	Quantity doubled to reflect use of two stacks in bus system
Hydrogen Piping	Piping and tubing diameters increased by a factor of 1.5 to adjust for higher hydrogen flow of bus system
System Controller	Quantity doubled to reflect increased control/sensors data channels in bus system
Current Sensors	Quantity doubled to reflect use of two stacks in bus system
Voltage Sensors	Quantity doubled to reflect use of two stacks in bus system
Hydrogen Sensors	One additional sensor added to passenger cabin to reflect much large volume of cabin in bus system
Belly Pan	Excluded from bus system since a dedicated, enclosed engine compartment is expected to be used
Mounting Frames	Size increased to reflect use of two stacks and larger BOP component in bus system
Wiring	Cost doubled to reflect use of two stacks in bus system
Wiring Fasteners	Cost doubled to reflect use of two stacks in bus system

Figure 32: Explanation of BOP component scaling for bus power plant

6.5 Bus System Vertical Integration

Vertical integration describes the extent to which a single company conducts many (or all) of the manufacturing/assembly steps from raw materials to finished product. High degrees of vertical integration can be cost efficient by decreasing transportation costs and turn-around times, and reducing nested layers of markup/profit. However, at low manufacturing rates, the advantages of vertical integration may be overcome by the negative impact of low machinery utilization or poor quality control due to inexperience/lack-of-expertise with a particular manufacturing step. Both the automotive and bus fuel cell power plants are currently cost modeled as if they are highly vertically integrated operations. While this is likely an appropriate assumption for the high manufacturing rates associated

with automobiles, it is more uncertain as applied to buses. Consequently, the issue of bus fuel cell power system vertical integration will be revisited in future analyses.

7 Capital and Quality Control Equipment

Quality control was introduced to the cost model beginning in the 2011 Report. Thus, the current auto and bus technology cost models include the cost of quality control equipment. The reader is referred to the 2011 Report for a detailed listing of quality control equipment for each manufacturing process.

For this effort, a complete review of the 2011 quality control was performed by team partners at NREL but was completed too late for changes to be implemented in the 2012 analysis. However, the review and suggestions will allow for further iteration and improved accuracy in modeling quality control equipment in the 2013 update to this modeling effort.

8 Automotive Simplified Cost Model Function

A simplified cost model to estimate the total automotive power system cost at 500,000 systems/year production rate is shown in Figure 33. The simplified model is based on key systems parameters likely to be readily available to the interested party and is generated from regression analysis of many runs of the full DFMA-style cost model. The simplified model allows a quick and convenient method to estimate system cost at off-baseline conditions.

A simplified cost model to estimate the total automotive power system cost at 500,000 systems/year production rate is shown in Figure 33. The simplified model splits the total system cost into five subcategories (stack cost, thermal management cost, water management cost, air management cost, and balance of plant cost) and generates a scaling equation for each one. The scaling equations for individual cost components are based on key system parameters for that component that are likely to be of interest when studying system scaling. The curves are generated by regression analysis of many runs of the full DFMA-style cost model over many variations of the chosen parameters. The simplified model allows a quick and convenient method to estimate system cost at off-baseline conditions.

C_{system} = Total System Cost = $C_{stack} + C_{thermal} + C_{water} + C_{air} + C_{BOP}$

C_{stack} = Total fuel cell stack cost

$250V\ C_{stack} = 3.67879E\text{-}05((3.8515E\text{-}08 \times A^2 + 0.0371 \times A - 1076.7099) \times L \times PC) + (0.0059818 \times A) + 331.4942$

$300V\ C_{stack} = 3.67879E\text{-}05((4.2201E\text{-}08 \times A^2 + 0.0349 \times A - 1177.6064) \times L \times PC) + (0.0062337 \times A) + 367.7989$

Where: A = Total active area of the stack (cm^2)
V= Stack Voltage
L = Pt Loading (mg/cm^2)
PC = Platinum cost ($/troy ounce)

C_{water} = Water Management System cost

$= (2.4424E\text{-}25 \times A^5 - 5.6171E\text{-}20 \times A^{3+} 5.1805E\text{-}15 \times A^4 - 2.4383E\text{-}10 \times A^3 + 6.1367E\text{-}06 \times A^2 - 0.07676 \times A - 399.46) + (51.684 \times (Q/\Delta T)/0.0920657) + 6.26$

Where: *A = Humidifier Membrane Area (cm^2)*
Q = Heat Duty for Precooler ($kW_{thermal}$)
ΔT = Difference between compressor exit air temperature and ambient temperature (°C)

$C_{thermal}$ = Thermal Management System cost

$= (111.351 \times Q_{HT}/\Delta T_{HT} + 184.116) + ((111.351 \times Q_{HT}/\Delta T_{HT} + 96.2938) \times Q_{LT}/Q_{HT})$

Where: *Q = Radiator Duty (ie. heat rejected from the stack) ($kW_{thermal}$)*
ΔT = Difference between stack operating temperature and ambient temperature (°C)
LT = Low Temperature Loop
HT = High Temperature Loop

C_{air} = Air Management System

$= (134.8044 \times P) + (1.07068 \times MF) + 101.024$

Where *P* = Air Peak Pressure (atm)
MF = Air Mass Flow (kg/hr)

C_{BOP} = Balance of Plant Cost

Where: $C_{BOP} = \$829.36$

Figure 33: Simplified automotive cost model

Because the simplified cost model equations are based upon regression analysis, there is a range of validity outside of which the values are not guaranteed to conform to the regression. The ranges for each parameter in each sub-equation are given in Figure 34 below.

Validity Range for Thermal Management System			
Parameter	Minimum Value	Maximum Value	Units
ΔT	40	70	°C
Q	100	325	kW_{gross}
Motor Power	100	600	W

Validity Range for Stack Cost			
Parameter	Minimum Value	Maximum Value	Units
System Power	60	120	kW_{net}
Platinum Loading	0.1	0.8	mg/cm^2
Total Active Area	70,000	165,000	cm^2
Platinum Cost	800	2,000	$/troy ounce

Validity Range for Air Management System			
Parameter	Minimum Value	Maximum Value	Units
Pressure	1.5	2.5	Atm
Air Mass Flow	300	650	kg/hr

Validity Range for Water Management System			
Parameter	Minimum Value	Maximum Value	Units
ΔT	40	80	°C
Q	1	10	kW
Membrane Area	20,000	60,000	cm^2

Figure 34: Range of validity for simplified cost model parameters

As a check on the accuracy of the simplified regression model, the results of the full DFMA model are compared to the calculations from the simplified model for the parameter of system net power. These results are displayed in Figure 35, indicating very good agreement between the two models within the range of validity.

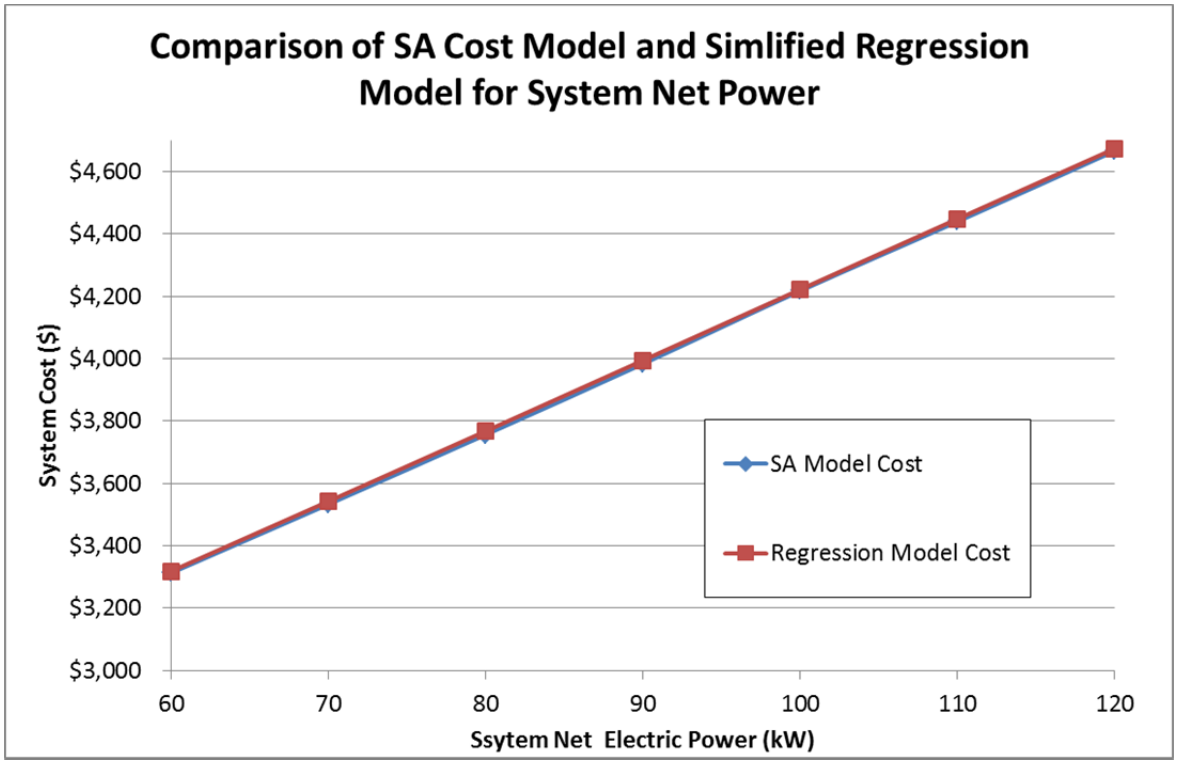

Figure 35: Comparison of SA cost model with simplified cost model

9 Lifecycle Cost Analysis

Up-front cost per kW, while a useful metric and the primary focus of this report, is not the sole determining factor in market worthiness of a power system. Total lifecycle cost is an equally important consideration that takes into account the initial purchase price, cost of fuel used over the lifetime of the system, system decommissioning costs and recycle credits, and operating and maintenance expenses, all discounted to the present value using a discounted cash flow methodology. By comparing lifecycle costs, it is possible to determine whether an inexpensive but inefficient system (low initial capital cost but high operating and fuel expenses) or an expensive but efficient system (high initial capital cost but low operating and fuel expenses) is a better financial value to the customer over the entire system lifetime.

The lifecycle analysis for this report assumes a set of driving conditions and platinum recycling costs to compute the total present value cost of ownership for the lifetime of the vehicle. These assumptions are summarized in the figure below.

Lifecycle Cost Assumption	Value
Sales markup	25% of calculated system cost
Discount rate	10%
System lifetime	10 years
Distance driven annually	12,000 miles
System efficiency at rated power	50% (calculated by model)
Fuel economy	65 mpgge[51]
Hydrogen to gasoline heating value ratio	1.011 kgH_2/gal gasoline
Fuel cost	\$5 / kg H_2
Total Pt loss during system lifetime and the Pt recovery process	10%
Market Pt price at end of system lifetime	\$1,100 / tr. oz.
Cost of Pt recovery	\$80 / tr. oz.
% of final salvaged Pt value charged by salvager	75%

Figure 36. Lifecycle cost assumptions

Many of the above assumptions are based upon adapting existing vehicular catalytic converter recycling parameters to expectations for a fuel cell system[,52,53]. Based on analysis of platinum recycling conducted by Mike Ulsh at the National Renewable Energy Laboratory, total platinum loss during operation and recovery is estimated at a 1% loss during operational life, 5% loss during recycling handing, and 2%-9% loss during the recycling process itself. 10% is chosen as the Pt loss baseline value while the low (8%) and high (15%) end are represented in the sensitivity analysis below. The cost of recycling[54] is expected

[51] Calculated from system efficiency at rated power based on formula derived from ANL modeling results: Fuel economy = 0.0028x^3 - 0.3272X^2+12.993X - 116.45, where x = system efficiency at rated power.
[52] "The impact of widespread deployment of fuel cell vehicles on platinum demand and price," Yongling Sun, et. al. International Journal of Hydrogen Energy 36 (2011).
[53] "Evaluation of a platinum leasing program for fuel cell vehicles," Matthew A. Kromer et. al., International Journal of Hydrogen Energy 34 (2009).
[54] Ibid.

to range between $75 and $90 per troy ounce of recovered platinum. However this is only the cost incurred by running the actual recycle process. In addition, there are supply chain costs as the capturer or salvager performing the recycle retains a portion of the value of the recovered metal. This is expected to be about 70%-75% of the total value of recycled platinum[55]. A sensitivity analysis is conducted for cases where the salvager captures only 35% of the recovered value. Finally, due to platinum market price volatility, it is unlikely that Pt price will be exactly the same at system purchase as it is 10 years later at time of recycle. Consequently, for purposes of the baseline LCC analysis, the price of platinum is held constant at the purchase price used for the catalyst within a new vehicle ($1,100 / tr. oz.), and sensitivity analysis is conducted for a future[56] higher Pt price ($2300/tr. oz. at end of life).

Under these assumptions, a basic set of cost results is calculated and displayed in Figure 37. Note that these results are only computed for the automotive system and not for the bus system; bus drive cycle and use patterns are vastly different from the average personal vehicle. Additional modeling and research is required to develop a representative equation governing the fuel economy of full-service transit buses.

	2012 Auto System Life Cycle Costs					
Annual Production Rate	**1,000**	**10,000**	**30,000**	**80,000**	**130,000**	**500,000**
System Cost	$17,403.83	$6,725.10	$5,668.96	$4,733.49	$4,410.57	$3,756.18
System Price (After Markup)	$21,754.79	$8,406.38	$7,086.20	$5,916.86	$5,513.21	$4,695.23
Annual Fuel Cost	$933.00	$933.00	$933.00	$933.00	$933.00	$933.00
Lifecycle Fuel Cost	$5,732.88	$5,732.88	$5,732.88	$5,732.88	$5,732.88	$5,732.88
Net Present Value of Recoverable Pt in System at End of System Lifetime	$200.05	$200.05	$200.05	$200.05	$200.05	$200.05
Final Pt Net Present Value Recovered	$50.01	$50.01	$50.01	$50.01	$50.01	$50.01
Total Lifecycle Cost	$27,437.66	$14,089.25	$12,769.07	$11,599.73	$11,196.08	$10,378.10
Total Lifecycle Cost ($/mile)	**$0.229**	**$0.117**	**$0.106**	**$0.097**	**$0.093**	**$0.086**

Figure 37: Auto LCC results for the baseline assumptions

The variation of lifecycle cost with system efficiency was studied in order to examine the trade-offs between low efficiency (higher operating costs but lower initial capital costs) and high efficiency (lower operating costs but higher initial capital costs) systems. Because the ANL 2012 performance optimization data was only obtained for 0.676 V/cell (and hence 55% fuel cell stack efficiency), the system performance as a function of cell voltage first had to be postulated. This was done by examining the shape of the polarization curve of 2011 ANL polarization data at 2012 operating conditions, and then shifting the curve appropriately for the changes between 2011 and 2012. The resulting comparison graph is shown Figure 38. The 2011 and 2012 ANL performance estimates (using 2012 conditions) are very similar. Consequently there is high confidence in the postulated 2012 polarization curve.

[55] Ibid.

[56] Platinum price is considered more likely to increase in the future rather than decrease. Consequently, the future price of Pt is based on the current Pt market price (~$1700/tr. oz) plus a $60/tr. oz. per year increase, resulting in a $2300/tr. oz. price after 10 years.

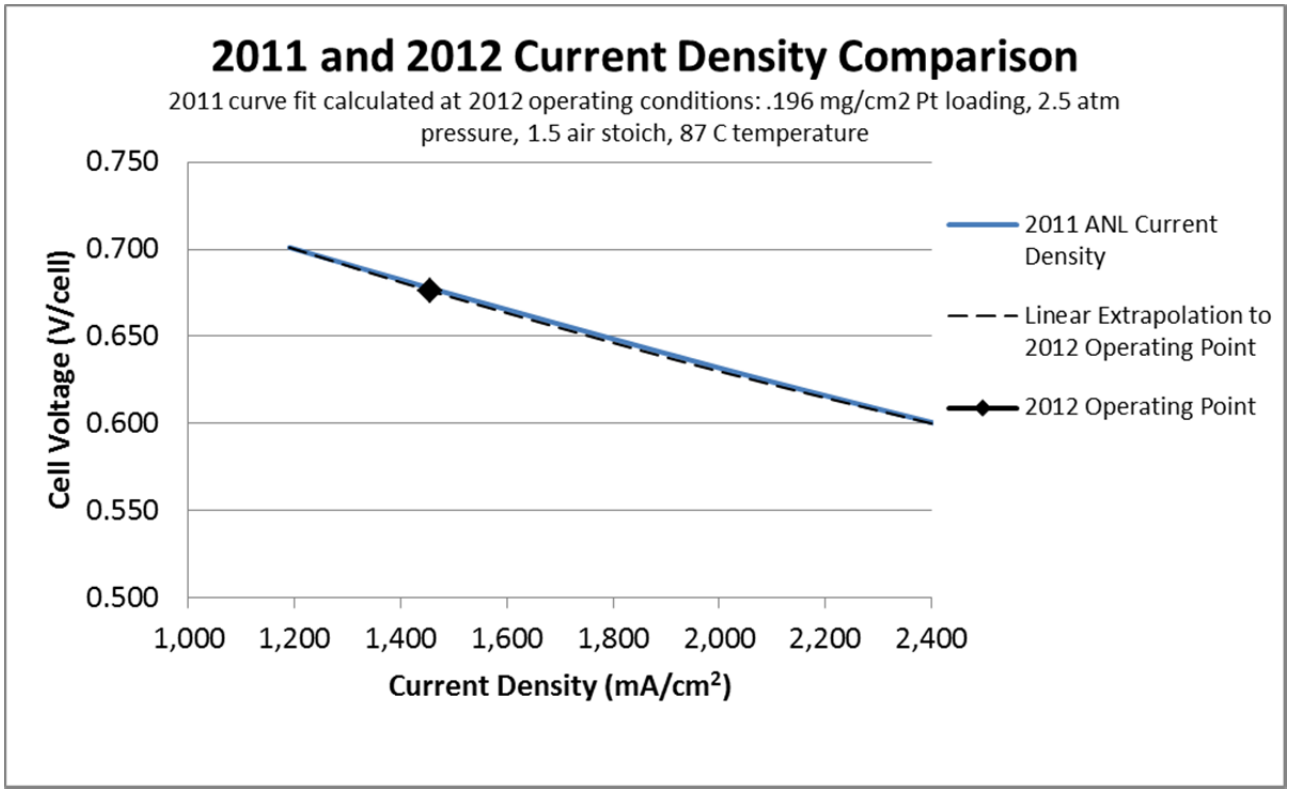

Figure 38: Polarization curves for efficiency sensitivity analysis

With this relationship, it is possible to calculate the variation in life cycle cost contributors over a range of efficiencies. These results are shown below. Figure 39 displays the results for the total lifecycle cost as well as its component costs on an absolute scale. Note that the total lifecycle cost (i.e. the present value of the 10 year expenses of the power system) is expressed as a $/mile value for easy comparison with internal combustion engine vehicle LCC analyses. Figure 40 shows a zoomed-in look at the total cost, indicating a minimum total life cycle cost at the baseline system value of 50% system efficiency (corresponding to 55% fuel cell stack efficiency and cell voltage of 0.676 V/cell). However, the range of LCC cost variation over the range of system efficiencies examined is quite small, indicating that LCC is generally insensitive to system efficiency.

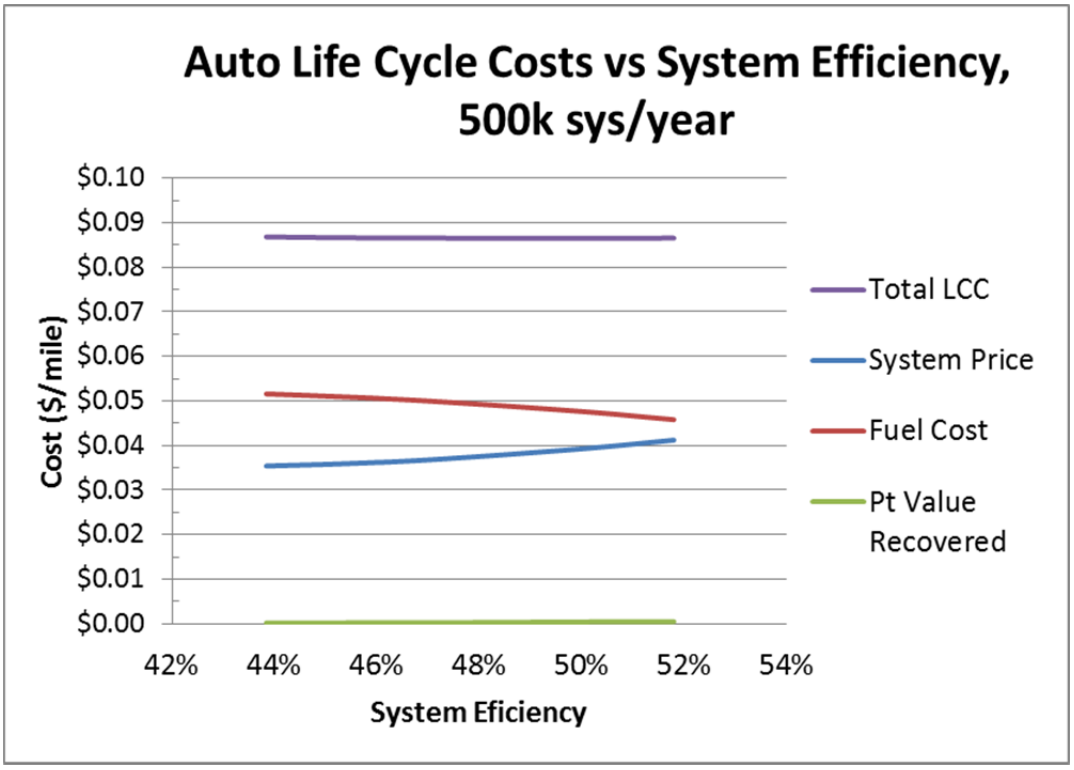

Figure 39: Life cycle cost components vs. fuel cell efficiency for 500k automobile systems/ year

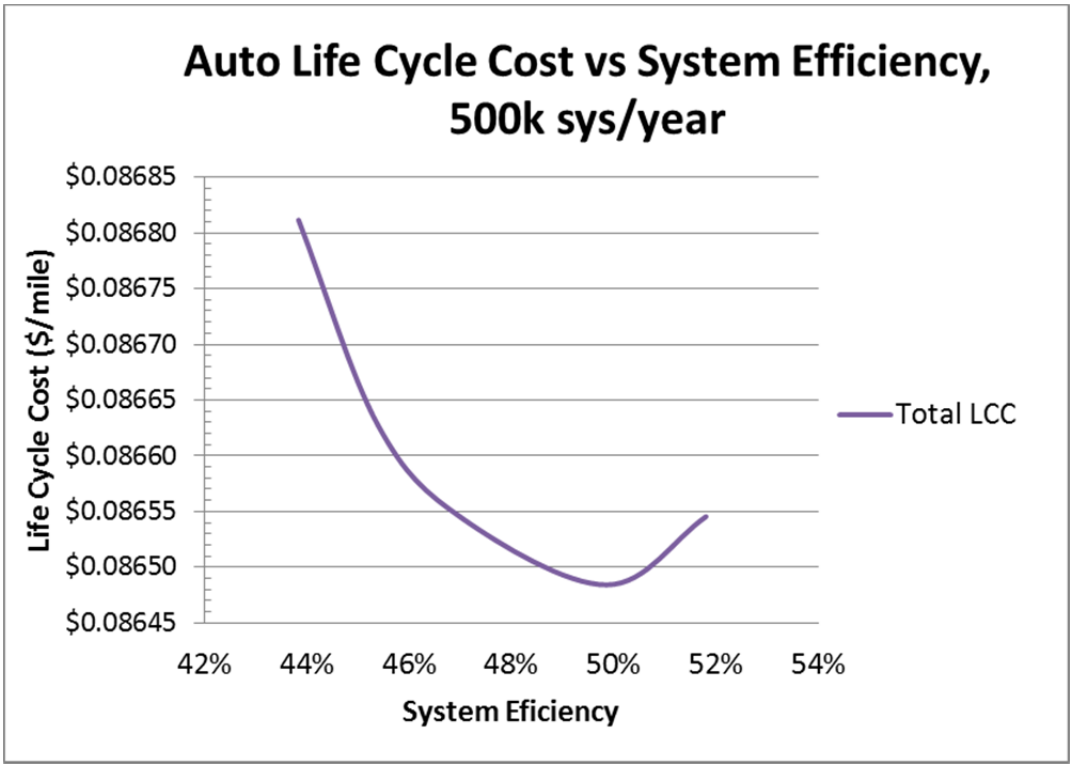

Figure 40: Life cycle cost vs. fuel cell efficiency for 500k automobile systems/year

In addition to the efficiency analysis, a simple sensitivity study was conducted on the parameters governing the platinum recycle, to determine the magnitude of the effect platinum recycling has on the lifecycle cost. Figure 41 below displays the total lifecycle cost in $ per mile as a function of platinum price during the year of the recycle for two scenarios: the baseline case where the recycler captures 75% of the value of recovered platinum and a sensitivity case where the recycler only captures 35% of the value.

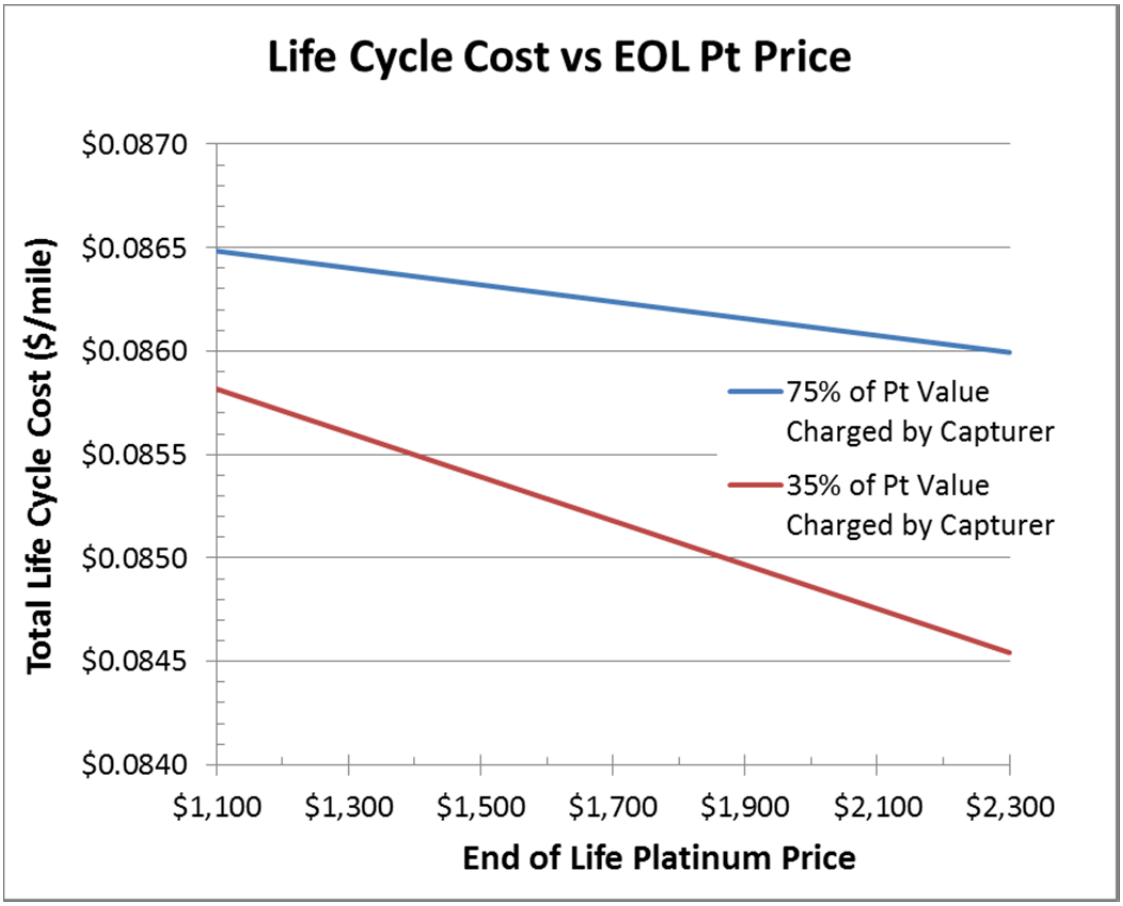

Figure 41: Life cycle cost vs. end of life platinum price (at 500k system/year)

Additional parameters were explored and are displayed as a tornado chart in Figure 42 and Figure 43. These results indicate that platinum recycle parameters do not have a large effect on the overall life cycle cost (~1%).

Life Cycle Cost ($/mile), 500,000 sys/year				
Parameter	**Units**	**Low Value of Variable**	**Base Value**	**High Value of Variable**
Salvage Value Charged		35%	**75%**	75%
Price at Recovery		$1,100	**$1,100**	$2,300
Total Pt Loss		8%	**10%**	15%
Cost of Recovery		$70	**$80**	$90
2012 Auto System LCC			**$0.08648**	

Figure 42: Life cycle cost tornado chart parameters

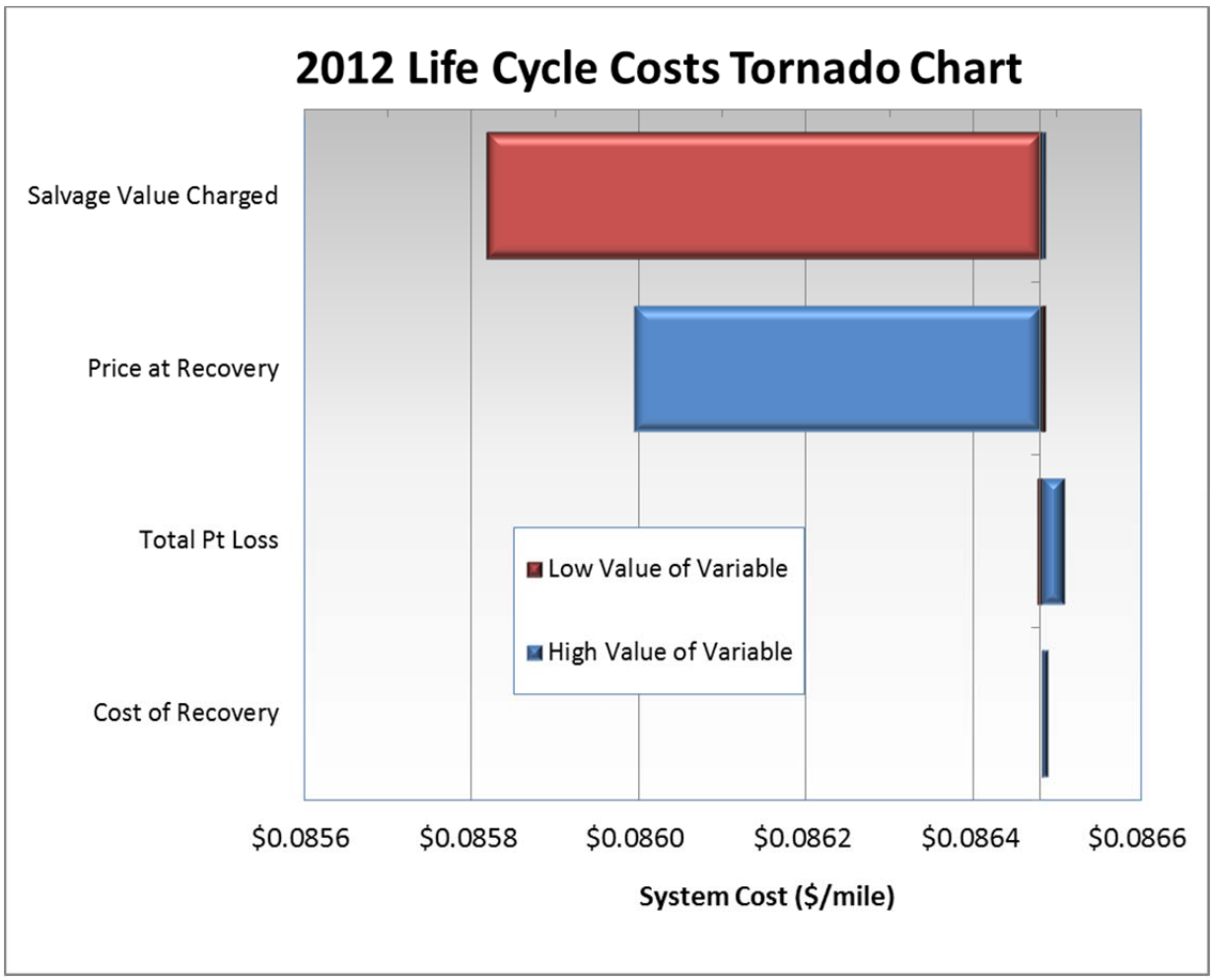

Figure 43: Life cycle cost tornado chart (at 500k systems/year)

10 Sensitivity Studies

A series of tornado and Monte Carlo sensitivity analyses were conducted to determine key parameters and assess avenues to further reduce cost.

10.1 Single Variable Analysis

10.1.1 Single Variable Automotive Analysis

A single variable analysis was performed to evaluate which parameters have the largest effect on system cost. Figure 44 shows the parameter ranges used to develop the tornado chart, while Figure 45 displays the results of the analysis.

System Cost ($/kWnet), 500,000 sys/year				
Parameter	**Units**	**Low Value**	**Base Value**	**High Value**
Power Density	**mW/cm^2**	233	**984**	1464
Pt Loading	**$mgPt/cm^2$**	0.15	**0.196**	0.3
Hydrogen Recirculation System Cost	**$/system**	$160.25	**$240.38**	$360.57
Compressor/Expander Efficiency Factor		0.90	**1**	1.03
Air Compressor Cost Factor		0.8	**1**	1
Bipolar Plate Cost Factor		1	**1.0**	1.5
Balance of Air Compressor Cost	**$/system**	$97.53	**$146.30**	$219.45
Ionomer Cost	**$/kg**	$45.65	**$75.06**	$148.55
GDL Cost	**$/$m^2$**	$3.23	**$4.45**	$5.80
Membrane Humidifier Cost	**$/system**	$52.94	**$52.94**	$100.00
2012 Auto System Cost				**$46.95**

Figure 44: 2012 Auto results tornado chart parameter values

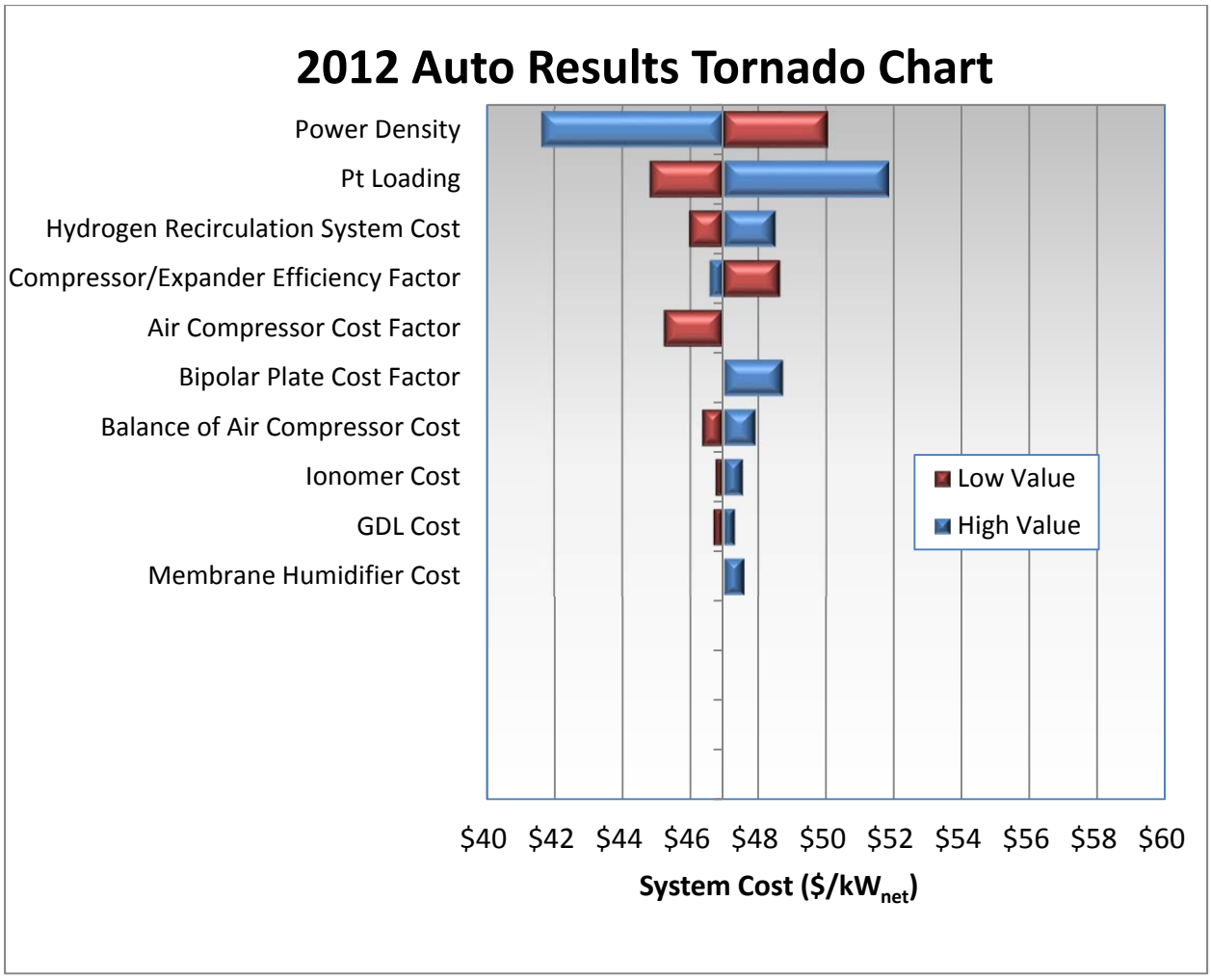

Figure 45: 2012 Auto results tornado chart

As shown in Figure 45, variations in operating condition parameters power density and platinum loading have the most capacity to affect system cost. For the case of power density, this affects the size and performance of the entire system, trickling down into cost changes in many components. Platinum loading's large effect is attributable to the very high price of platinum relative to the quantities used in the system.

10.1.2 Automotive Analysis at a Pt price of $1550/troy ounce

To aid in comparisons to other cost studies, the automotive system was also evaluated with a platinum price of $1,550/troy ounce (instead of the baseline value of $1,100/troy ounce). All other parameters remain the same. Results are shown in Figure 46.

	2012 Automotive System					
Annual Production Rate	**1,000**	**10,000**	**30,000**	**80,000**	**130,000**	**500,000**
System Net Electric Power (Output)	80	80	80	80	80	80
System Gross Electric Power (Output)	88.24	88.24	88.24	88.24	88.24	88.24
Fuel Cell Stacks	$12,030.41	$3,595.59	$2,648.64	$2,262.84	$2,143.33	$1,912.74
Balance of Plant	$5,527.67	$3,328.28	$3,220.79	$2,671.34	$2,468.38	$2,044.57
System Assembly & Testing	$145.13	$100.62	$98.90	$98.69	$98.24	$98.25
Total System Cost ($)	$17,703.21	$7,024.49	$5,968.34	$5,032.87	$4,709.94	$4,055.56
Total System Cost ($/kW$_{net}$)	$221.29	$87.81	$74.60	$62.91	$58.87	$50.69
Total System Cost ($/kW$_{gross}$)	$200.62	$79.60	$67.64	$57.03	$53.38	$45.96

Figure 46: Detailed system cost for the 2012 automotive technology system with a Pt price of $1,550/troy ounce

10.1.3 Single Variable Bus Analysis

A single variable analysis of the bus system was also conducted. Because 1,000 systems/year is the only manufacturing rate analyzed for the bus, the cost at this rate is the cost considered.

System Cost ($/kWnet), 1,000 sys/year				
Parameter	**Units**	**Low Value**	**Base Value**	**High Value**
Power Density	**mW/cm^2**	500	**716**	984
Pt Loading	**mgPt/cm^2**	0.2	**0.4**	0.8
GDL Cost	**$/m^2**	$74.10	**$115.87**	$151.02
Bipolar Plate & Coating Cost Factor		1	**1**	2
Air Compressor Cost Factor		0.8	**1**	1
Membrane Humidifier Cost	**$/system**	$382.83	**$765.66**	$1,531.32
Ionomer Cost	**$/kg**	$45.65	**$204.00**	$500.00
Hydrogen Recirculation System Cost	**$/system**	$321.00	**$641.99**	$1,283.98
Balance of Air Compressor Cost	**$/system**	$185.25	**$370.50**	$741.00
Product of Compressor / Motor & Motor Controller Efficiencies	**%**	51%	**59%**	64%
2012 Bus System Cost				**$190.69**

Figure 47: 2012 Bus results tornado chart parameter values

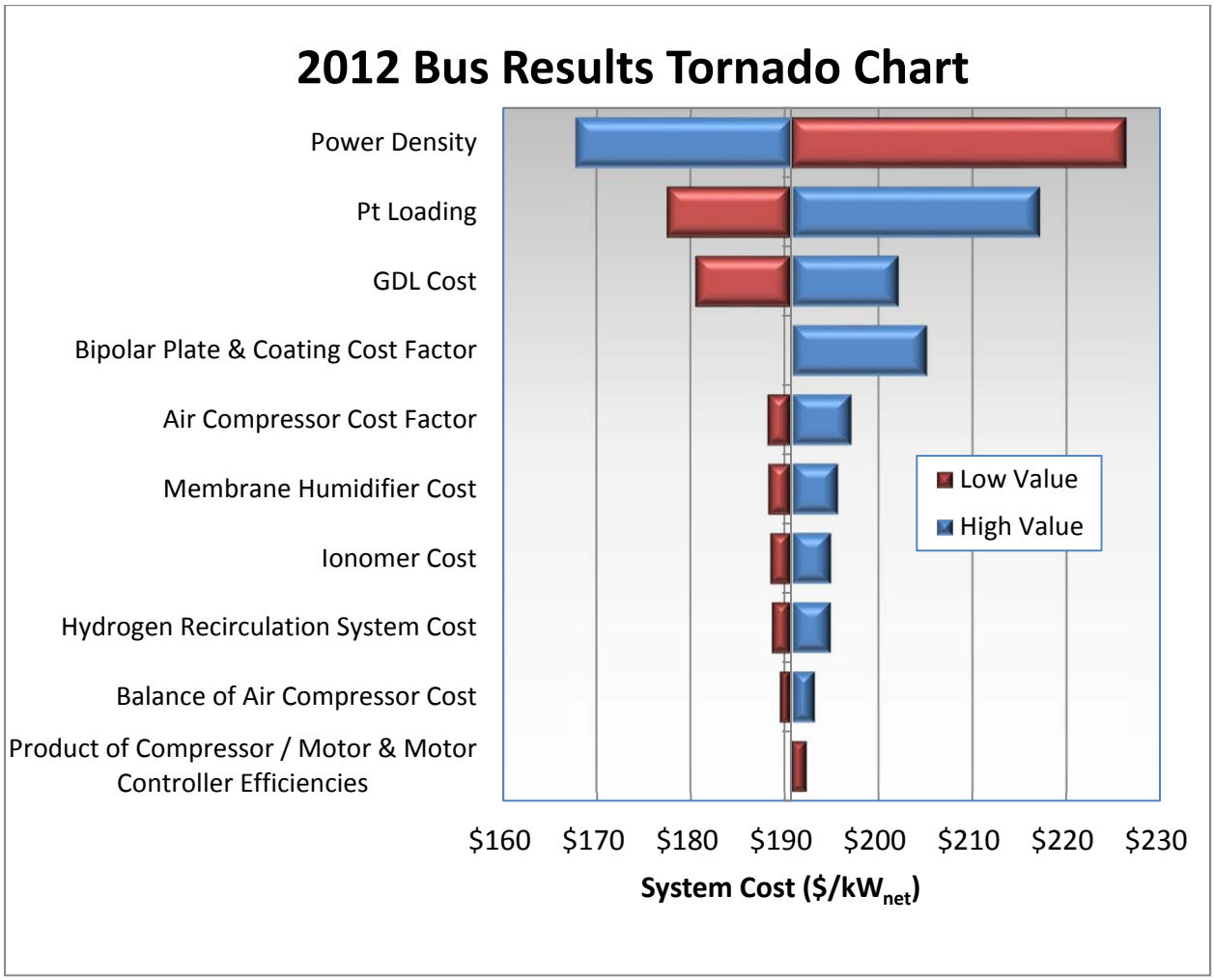

Figure 48: 2012 Bus results tornado chart

As with the automotive system, power density and platinum loading have the largest potential to vary system cost. Unlike the automotive system, however, there is also a large cost variation potential to be found in GDL and bipolar plate cost variations. This is because at lower manufacturing rate, the cost of manufactured component items is high and subject to large changes in cost relative to components manufactured at high volume, as in the automotive case.

10.2 Monte Carlo Analysis

In order to evaluate the bounds for the likely variation in final results, a Monte Carlo analysis was conducted for both the automotive and bus results. With these results, it is possible to examine the probability of various model outcomes based upon assumed probability functions for selected inputs. For all inputs, triangular distributions were chosen with a minimum, maximum, and most likely value. The most likely value is the result used in the baseline cost analysis, while the maximum and minimum were chosen with the input of the Fuel Cell Tech Team to reflect likely real-world bounds for 2012.

10.2.1 Monte Carlo Automotive Analysis

Assumptions and results for the Monte Carlo analysis of the automotive system at a manufacturing rate of 500,000 systems/year are shown in Figure 49 and Figure 50.

2012 Technology Monte Carlo Analysis, 500k sys/year				
Parameter	**Unit**	**Minimum Value**	**Likeliest Value**	**Maximum Value**
Power Density	**mW/cm2**	833	**984**	1464
Pt Loading	**mgPt/cm2**	0.15	**0.196**	0.3
Ionomer Cost	**$/kg**	$45.65	**$75.06**	$148.55
GDL Cost	**$/m2**	$3.23	**$4.45**	$5.80
Bipolar Plate & Coating Cost Factor		1	**1**	1.5
Membrane Humidifier Cost	**$/system**	$52.94	**$52.94**	$100.00
Product of Compressor / Expander / Motor & Motor Controller Efficiencies		0.415	**0.51**	0.54
Air Compressor Cost Factor		0.8	**1**	1
Balance of Air Compressor Cost	**$/system**	$97.53	**$146.30**	$219.45
Hydrogen Recirculation System Cost	**$/system**	$160.25	**$240.38**	$360.57

Figure 49: 2012 automotive Monte Carlo analysis bounds

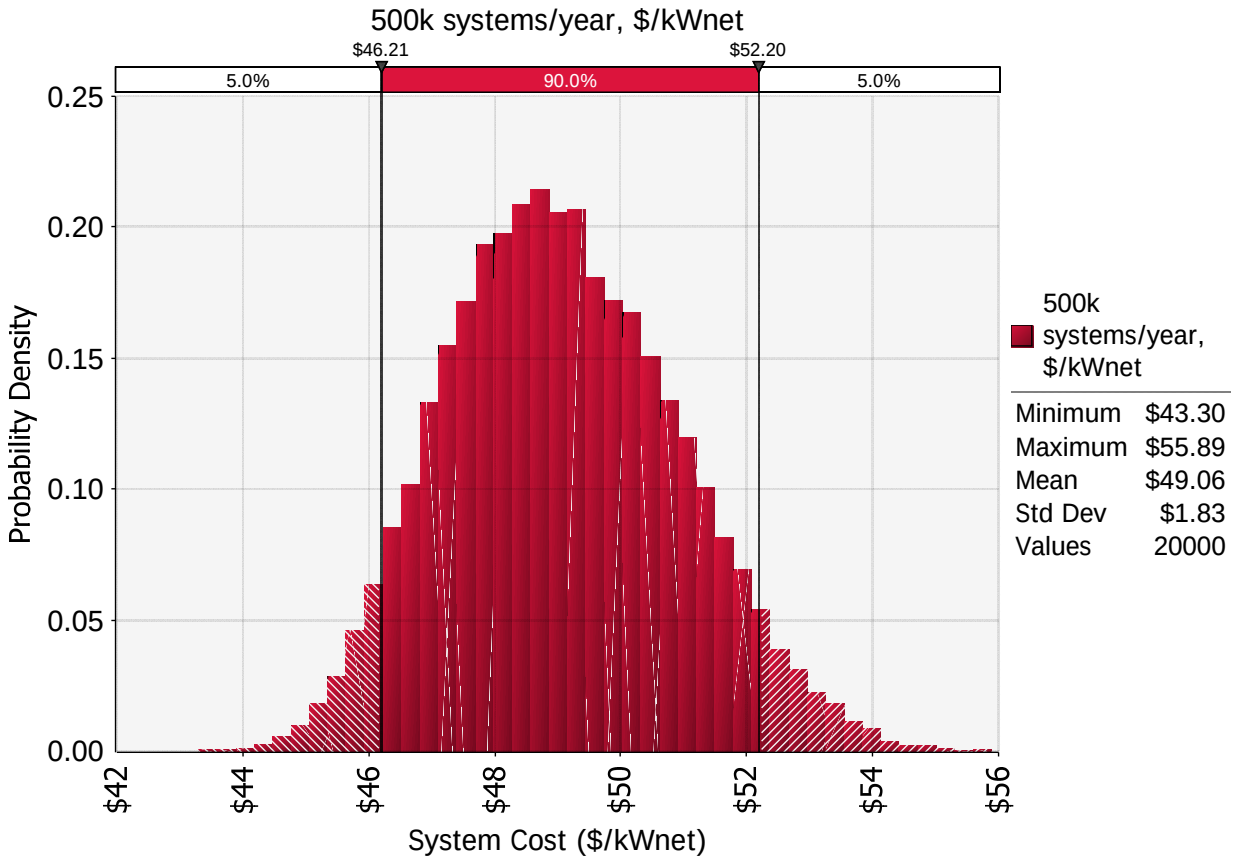

Figure 50: 2012 automotive Monte Carlo analysis results

Monte Carlo analysis indicates that the middle 90% probability range of cost is between \$46.21/kW_{net} and \$52.20/kW_{net} for the automotive system at 500,000 systems/year.

10.2.2 Monte Carlo Bus Analysis

Assumptions and results for the Monte Carlo analysis of the bus system at a manufacturing rate of 1,000 systems/year are shown in Figure 51 and Figure 52Figure 50.

2012 Bus Technology Monte Carlo Analysis, 1k sys/year				
Parameter	**Unit**	**Minimum Value**	**Likeliest Value**	**Maximum Value**
Power Density	**mW/cm2**	500	**716**	984
Pt Loading	**mgPt/cm2**	0.2	**0.4**	0.8
Ionomer Cost	**$/kg**	$45.65	**$204.00**	$500.00
GDL Cost	**$/m2**	$84.10	**$115.87**	$151.02
Bipolar Plate & Coating Cost Factor		1	**1**	2
Membrane Humidifier Cost	**$/system**	$382.83	**$765.66**	$1,531.32
Product of Compressor / Expander / Motor & Motor Controller Efficiencies		0.510	**0.588**	0.64
Air Compressor Cost Factor		0.8	**1**	1.5
Balance of Air Compressor Cost	**$/system**	$185.25	**$370.50**	$741.00
Hydrogen Recirculation System Cost	**$/system**	$321.00	**$641.99**	$1,283.98

Figure 51: 2012 bus Monte Carlo analysis bounds

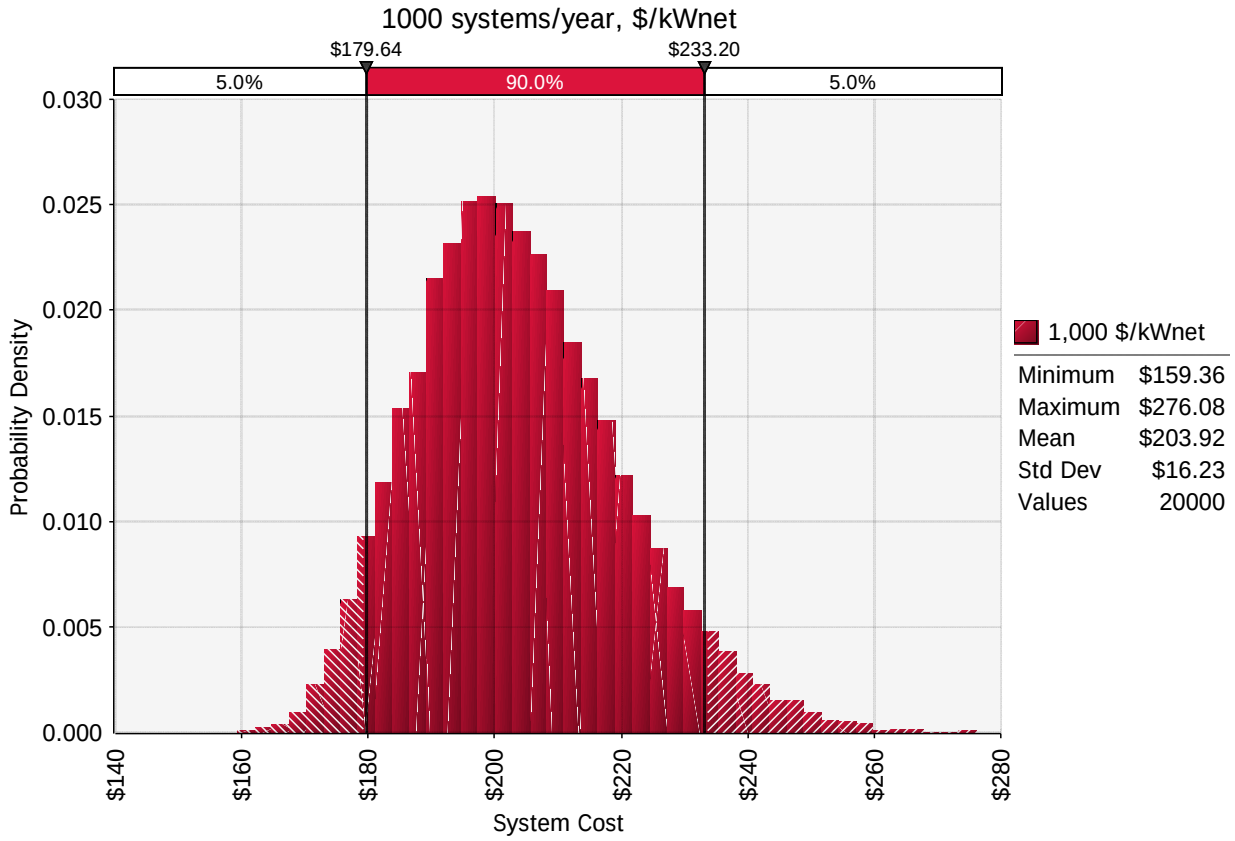

Figure 52: 2012 bus Monte Carlo analysis results

Monte Carlo analysis indicates that the middle 90% probability range of cost is between $179.64/kW$_{net}$ and $233.20/kW$_{net}$ for the bus system at 1,000 systems/year.

10.3 Analysis of Bus Operation at Higher Pressure with an Exhaust Gas Expander

The baseline bus power system operates at 1.8 atm under design conditions with this pressurization level chosen to match current Ballard bus fleet practice. However, the automotive power system pressure is selected not by imitation of current practice but by cost optimization. Consequently, a similar system level cost optimization was conducted for the bus system to determine the operating pressure (and presence or absence of an expander) that leads to lowest system cost. Results of the optimization are shown in Figure 53 and reveal that a 2.5 atm pressure with an exhaust gas expander results in the lowest system cost. However, the difference between the compressor-only and the compressor-with-expander case is surprisingly small, suggesting that the compressor-only case may reasonably be chosen since it is mechanically less complex. Both curves have a moderate slope, suggesting that increased pressure is preferred as the higher power density afforded by increased pressure more than compensates for the higher system gross power resulting from higher compression parasitics. The optimization is based on 2012 ANL stack modeling which is limited to 2.5 atm. However both curves are observed to be leveling out with increasing pressure, suggesting that only minor gains may be attained at pressure above 2.5 atm. Overall, the sensitivity analysis suggests that system cost might be reduced by ~9% (from $191/kWnet to $174/kWnet) by increasing pressure from 1.8 atm to 2.5 atm. However, this cost improvement must be balanced against several factors not reflected in the analysis: potential for increased cell gas leakage, enhanced stack compression requirements, and potential difficulties/risks in handling the higher air temperatures resulting from higher compression ratio.

(Note that stack polarization performance for the optimization is based on 2012 ANL modeling of 3M NSTF MEA performance for 0.196mgPt/cm^2 but with catalyst loading increased to 0.4mgPt/cm^2 for cost purposes only. This is to model an optimized high-durability and high-performance MEA suitable for bus application. Durability and performance at this loading has not been experimentally demonstrated.)

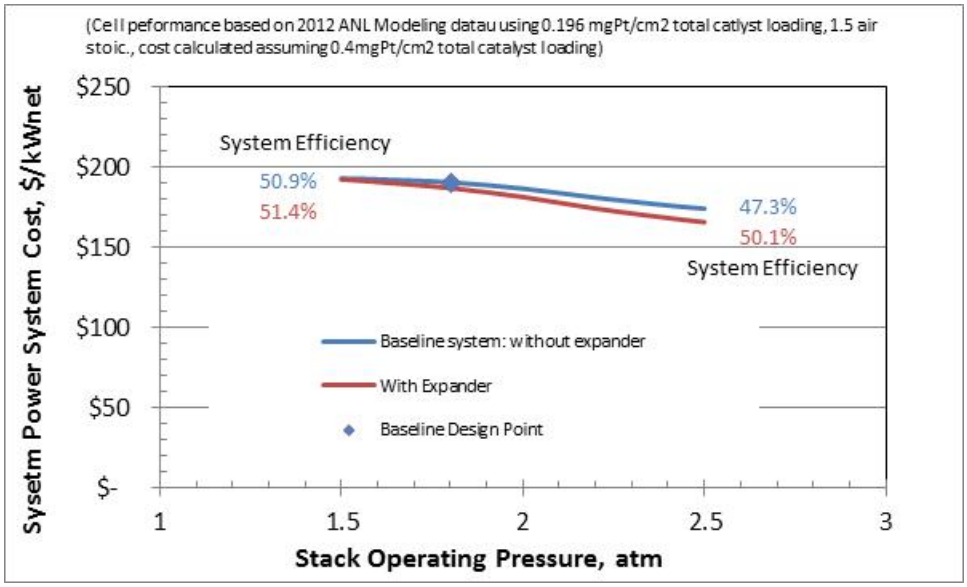

Figure 53: Bus pressure optimization for lowest system cost

11 Summary Observations of the 2012 Automotive and Bus Analyses

Summary observations appear below for both the automotive and bus power systems.

<u>80kW net electric light-duty automotive fuel cell power systems:</u>

- The 2011 DFMA-style cost analysis was updated to reflect changes/improves achieved in 2012.
- Performance is based on an updated 2012 stack polarization model provided by Argonne National Laboratory (based on recent 3M nanostructured thin-film (NSTF) catalyst test data).
- The 2012 system is optimized for low cost: the optimized operating conditions slightly differ from the 2011 optimization conditions.

	2011 Design Point	**2012 Design Point**
Cell voltage	0.676 volts/cell	0.676 volts/cell
Power density	1,100 mW/cm^2	984 mW/cm^2
Pressure	3.0 atm	2.5 atm
Total catalyst loading	0.186 mgPt/cm^2	0.196 mgPt/cm^2
Stack Temperature	95°C	87°C
Cathode Air Stochiometry	1.5	1.5

- The 2012 stack operating pressure was lowered to 2.5 atm primarily due to that being the upper limit of available polarization data. Further system cost decreased with increases in pressure are suggested but not demonstrated (due to the limited data set).
- Other significant changes for 2012 include: improved ionomer cost estimates, improved GDL cost estimates, use of sub-gaskets for MEA sealing (as opposed to the 2011 method of frame-gaskets), and several other minor alterations.
- The final 2012 automobile cost was \$46.95/kW$_{net}$ at 500,000 systems/year.

- Monte Carlo analysis yields middle 90% probability bounds of \$46.21/kW_{net}-\$52.20/kW_{net} for the automotive system.
- The 2012 automobile system balance of plant (BOP) components represent 54% of the overall system cost.

160kW Bus fuel cell power systems:

Stack performance is based on 2012 stack polarization model provided by Argonne National Laboratory (the same data set used for the automotive system) but with total Pt loading raised from 0.196 $mgPt/cm^2$ to 0.4$mgPt/cm^2$ to reflect the longer durability requirements of the bus application.

- Power density, voltage, pressure, and catalyst loading of the selected system design point is consistent with the actual operating conditions of Ballard fuel cell buses currently in service.

	Approximate Ballard Bus Design Point	**2012 Bus Design Point**
Cell voltage	~0.69 volts/cell	0.676 volts/cell
Power density	~759 mW/cm^2	716 mW/cm^2
Pressure	~1.8 atm	1.8 atm
Total catalyst loading	~0.4 $mgPt/cm^2$	0.4 $mgPt/cm^2$
Stack Temperature	~60°C	74°C
Cathode Air Stochiometry	1.5-2.0	1.5

- Primary differences between the bus and auto power systems are: system power (160kW vs. 80kW), number of stacks (two vs. one), operating pressure (1.8 atm vs. 2.5 atm), catalyst loading (0.4 $mgPt/cm^2$ vs. 0.196 $mgPt/cm^2$), use of an exhaust gas expander (no expander vs. expander), type of air compressor (twin vortex vs. centrifugal).
- The system schematics and stack construction are nearly identical between the bus and automobile systems.
- The final 2012 bus cost was \$190.69/kW_{net} at 1,000 systems/year.
- Monte Carlo analysis yields middle 90% probability bounds of \$179.64/kW_{net}-\$233.2/kW_{net} for the bus system.
- The 2012 bus system BOP represented only 29% of the overall system cost
- Because fewer bus systems are produced in a year at maximum rate, bus system costs are much more sensitive than automobile costs to variations in the cost of components such as GDL or bipolar plate manufacturing.
- Sensitivity analysis suggests very little cost improvement is achieved with the use of an exhaust gas expander.
- Sensitivity analysis suggests that ~9% system cost savings might be achieved by operating at a higher pressure (up to 2.5 atm).